nature communications

Article

https://doi.org/10.1038/s41467-024-52807-3

A sexually transmitted sugar orchestrates reproductive responses to nutritional stress

Received: 2 February 2024

Accepted: 19 September 2024

Published online: 01 October 2024

Check for updates

Seong-Jin Kim[1,6], Kang-Min Lee[1,6], Si Hyung Park[2], Taekyun Yang[1], Ingyu Song[1], Fumika Rai[3], Ryo Hoshino[3], Minsik Yun[1], Chen Zhang[1], Jae-Il Kim[1], Sunjae Lee[1], Greg S. B. Suh[4], Ryusuke Niwa[5], Zee-Yong Park[1] & Young-Joon Kim[1]

Seminal fluid is rich in sugars, but their role beyond supporting sperm motility is unknown. In this study, we found *Drosophila melanogaster* males transfer a substantial amount of a phospho-galactoside to females during mating, but only half as much when undernourished. This seminal substance, which we named venerose, induces an increase in germline stem cells (GSCs) and promotes sperm storage in females, especially undernourished ones. Venerose enters the hemolymph and directly activates nutrient-sensing Dh44^{+} neurons in the brain. Food deprivation directs the nutrient-sensing neurons to secrete more of the neuropeptide Dh44 in response to infused venerose. The secreted Dh44 then enhances the local niche signal, stimulating GSC proliferation. It also extends the retention of ejaculate by females, resulting in greater venerose absorption and increased sperm storage. In this study, we uncovered the role of a sugar-like seminal substance produced by males that coordinates reproductive responses to nutritional challenges in females.

Seminal fluid serves as a medium for sperm transport, yet its biological functions extend far beyond this role. In humans, nearly 10,000 peptides or proteins are found in seminal fluid or are associated with sperm. These are involved in a variety of molecular and cellular changes that occur in inseminated females, including uterine inflammatory responses, preparation of the uterine endometrium, and facilitation of preimplantation[1,2]. In addition to peptides and proteins, seminal fluid also contains a substantial amount of fructose[3]. Fructose is recognized as an energy source for sperm motility and is a clinically important indicator of male fertility[4].

The fruit fly *Drosophila melanogaster* has emerged as a valuable model for unravelling the functions of seminal fluid proteins in female reproduction and sexual selection[5,6]. For example, several studies have focused on the seminal fluid component sex peptide (SP). SP is produced by the male accessory gland (MAG), which is analogous to the mammalian prostate. Upon insemination, SP enters the hemolymph and triggers a wide range of changes to female reproductive physiology and post-mating behaviors[7–9]. Like that of mammals, insect seminal fluid also contains free sugars[3]. But beyond their role as an energy source for sperm motility, the signaling functions of these sugars remain unknown.

Mating stimulates egg laying and increases egg production. SP enhances oogenesis progression by fostering the development of pre-vitellogenic follicles into vitellogenic follicles[10–12]. Moreover, SP is implicated in the generation of pre-vitellogenic follicles by inducing the proliferation of germline stem cells (GSCs). GSCs, located in the foremost region of each ovariole of the germarium in *Drosophila*, are vital for the continuous production of gametes[13]. The transient increase in GSCs induced by SP is achieved through the participation of various endocrine or paracrine factors, including ecdysteroids (20E) and octopamine (OA) from the ovary, and neuropeptide F (NPF) from the gut[10,14,15].

[1]School of Life Sciences, Gwangju Institute of Science and Technology, Gwangju 61005, Republic of Korea. [2]School of Horticulture and Forestry, College of Bio and Medical Sciences, Mokpo National University, Muan 58554, Republic of Korea. [3]Graduate School of Science and Technology, University of Tsukuba, Tsukuba, Ibaraki 305-8572, Japan. [4]Department of Biological Sciences, Korea Advanced Institute of Science and Technology, Daejeon 34141, Republic of Korea. [5]Life Science Center for Survival Dynamics, Tsukuba Advanced Research Alliance (TARA), University of Tsukuba, Tsukuba, Ibaraki 305-8577, Japan. [6]These authors contributed equally: Seong-Jin Kim, Kang-Min Lee. e-mail: kimyj@gist.ac.kr

Courtship feeding is prevalent across taxa[16–18], and in extreme cases, mating induces some female insects to feed on male body parts[19,20]. *Drosophila* exemplifies another form of courtship feeding referred to as seminal feeding, whereby males transfer nutrient-rich seminal fluids to their mates[21,22]. In general, courtship feeding promotes male paternity because females typically prefer gift-giving males. Courtship feeding and food quality are positively correlated with copulation duration, allowing for more sperm transfer[23–25]. There is also a clear link between courtship feeding and postcopulatory sexual selection[26,27]. For instance, in the nursery web spider *Pisaura mirabilis*, females preferentially store more sperm from food gift-giving males than those offering no gift[28].

Preferential sperm uptake has been observed in various animal species, often occurring via an alteration of the delay between copulation and sperm ejection (expulsion), namely the ejaculate holding period (EHP)[29]. EHP length determines the amount of sperm stored, with longer EHPs resulting in more sperm storage[30,31]. Sperm ejection after a very short EHP was first observed in dunnock females mated with subdominant males[32]. Since then, similar phenomena have been documented in many birds and insects including *Drosophila*[33,34].

Fruit flies exhibit various EHP durations, and one molecular genetic study identified a brain pathway that regulates the timing of sperm ejection and therefore EHP. This brain pathway, comprising the neuropeptide diuretic hormone 44 (Dh44) and its GPCR receptor Dh44-R1, is essential for establishing a normal EHP[31]. Loss of Dh44 or its receptor results in precocious sperm ejection, leading to a shortened EHP and reduced sperm uptake. Intriguingly, the brain neurosecretory cells that produce Dh44 and regulate EHP (i.e., the Dh44-PI neurons) sense circulating sugars in the internal milieu[35,36]. These discoveries raise the intriguing possibility that Dh44-PI neurons are involved in assessing courtship feeding and adjusting sperm uptake accordingly.

Here, we identified venerose, a small sugar-like substance abundant in seminal fluid, that affects GSC proliferation and preferential sperm uptake. Upon insemination, seminal venerose enters the female hemolymph, activating the brain Dh44-PI neurons and triggering their secretion of Dh44. Then, Dh44 in the hemolymph stimulates GSC proliferation by elevating local GSC niche signals. The transfer of venerose from males to females could be considered a form of courtship feeding, as venerose serves as the primary source of elemental phosphorus females absorb from the male ejaculate. In energy-deprived females, Dh44-PI neurons respond to venerose by releasing a larger amount of Dh44, leading to a prolonged EHP, increased venerose absorption, and enhanced sperm storage. Importantly, this process enables females to assess the energy levels of their mates. Under energy-deprived conditions, males decrease venerose production by approximately half. Consequently, females paired with these energy-deprived males secrete less Dh44 compared to their counterparts mating with well-nourished males, resulting in a shorter EHP and reduced sperm storage. These findings reveal a intersexual signaling pathway that is sensitive to nutritional status, suggesting its role in optimizing reproductive outcomes and influencing sexual selection during nutritional challenges.

Results

Venerose, a phospho-galactoside abundant in seminal fluid

We employed mass spectrometry to identify sugars in male ejaculate but found no evidence of mass units corresponding to glucose, trehalose, or fructose. Instead, we observed a robust signal at a molecular weight of 377, $[M\text{-}H]^-$ = 376.10142 (Fig. 1a). In subsequent examinations of male and female reproductive tissue extracts, we found this peak was present exclusively in males and primarily localized to the MAG, the major source of seminal fluid substances (Fig. 1b, Supplementary Fig. 1). Hereafter, we will refer to this substance as the *Drosophila* venereal sugar or venerose. Venerose was the major peak in the hydrophilic eluent of MAG extracts (Fig. 1b), with trace amounts also present in male ejaculatory ducts and testes (Fig. 1c).

After deducing the molecular formula of venerose—$C_{11}H_{24}O_{11}NP$—via electrospray ionization high-resolution mass spectrometry ($[M\text{-}H]^-$ $C_{11}H_{23}O_{11}NP^-$, calculated *m/z* 376.10142, found 376.10139, Δ 0.08 ppm mass error), we proceeded to a structural identification via ^1H, ^{13}C, and ^{31}P NMR and 2D NMR spectral analyses (Supplementary Table 1; Supplementary Fig. 2). The combined ^1H-^1H COSY, ^{13}C-^1H HMQC, and HMBC spectra revealed the structure of venerose as 1-*O*-[4-*O*-(2-aminoethylphosphate)-β-$_D$-galactopyranosyl]-x-glycerol (Fig. 1d). Although this sugar was previously identified in *D. melanogaster* male accessory glands, it had not yet been associated with a biological function[37]. Our ^{31}P-NMR analysis of the MAG extracts indicated that a single male fly produces approximately 0.45 μg or 1.2 nmol of venerose. In a single mating, the male transfers 39 ± 3.6% of its venerose pool to the female, after which it restores its venerose pool within approximately 24 h (Fig. 1e).

Glucosyltransferase is required for venerose production

In a search for genes involved in venerose biosynthesis, we identified several mutants with transposons inserted in genes encoding enzymes involved in diacylglycerol biosynthesis (Supplementary Fig. 3a–c). The MAG is rich in lipids and lipases[38], and we found that RNAi-mediated knockdown of specific lipases in the MAG significantly reduced venerose production (Supplementary Fig. 3d). Venerose carries a β-galactose attached to glycerol, a moiety commonly found in glycoglycerolipids. This suggests venerose production requires a glycosyltransferase capable of transferring galactose or other hexoses to a lipid acceptor with a glycerol moiety (e.g., diacylglycerol). Thus, we searched the Carbohydrate-Active enZymes (CAZy) database[39,40] and found that the GT28 gene family has 1,2-diacylglycerol 3-β-galactosyltransferase activity[41] (Supplementary Data 1). The *D. melanogaster* genome contains 18 genes with a GT28 domain, 6 of which are expressed in the MAG (Fig. 2a; Supplementary Data 2 and Table 2). By performing MAG-specific RNAi knockdown, we found that knockdown of *UGT305A1*, *UGT302C1*, *UGT304A1*, or *UGT37D1* each significantly reduced venerose levels (Fig. 2b; Supplementary Fig. 3e). This result suggests these enzymes contribute with some redundancy to venerose production. The MAG matures over 4–5 days after emergence[42], and although the MAG contains minimal venerose at emergence, its venerose pool increases rapidly post-emergence (Supplementary Fig. 3f). We found UGT305A1 expression in the MAG increases during this period (Fig. 2a; Supplementary Table 2). We also found overexpression of UGT305A1 in the MAG increased venerose production by 33–40% compared to controls (Fig. 2c). *UGT305A1* knockdown, however, did not significantly affect the size or shape of the MAG, nor did it affect its content of other seminal substances such as SP (Supplementary Fig. 4). Therefore, in subsequent experiments, we used *UGT305A1* knockdown males as venerose-deficient males.

We analyzed single-nucleus transcriptome data to examine the spatial expression patterns of genes involved in venerose biosynthesis, including GT28, lipase, and DAG metabolism genes[43]. We focused our analysis on the male reproductive tract, where the *prd* gene, from which the *Prd-F-Gal4* transgene used to drive GT28 knockdown is derived, is predominantly expressed (Supplementary Fig. 4f). In contrast to our bulk RNA-seq result showing significant expression of Ugt305A1 and related GT28 genes required for venerose synthesis (Fig. 2a; Supplementary Table 2), our single-nucleus RNA-seq analysis did not identify any MAG cells expressing these genes. This is likely because the MAGs used in the single-cell RNA-seq analysis had low expression at the time of sampling (i.e., 2–3-day-old males), as the expression of these genes increases transiently after eclosion. Although we did find that certain cell types, such as spermatocytes, produce a subset of these genes, we were unable to identify a cell type that produces all the required venerose genes. This suggests venerose biosynthesis may require the cooperative action of cells derived not only from the male reproductive tract but also from other metabolically relevant tissues (e.g., gut, fat body, etc.).

https://doi.org/10.1038/s41467-024-52807-3

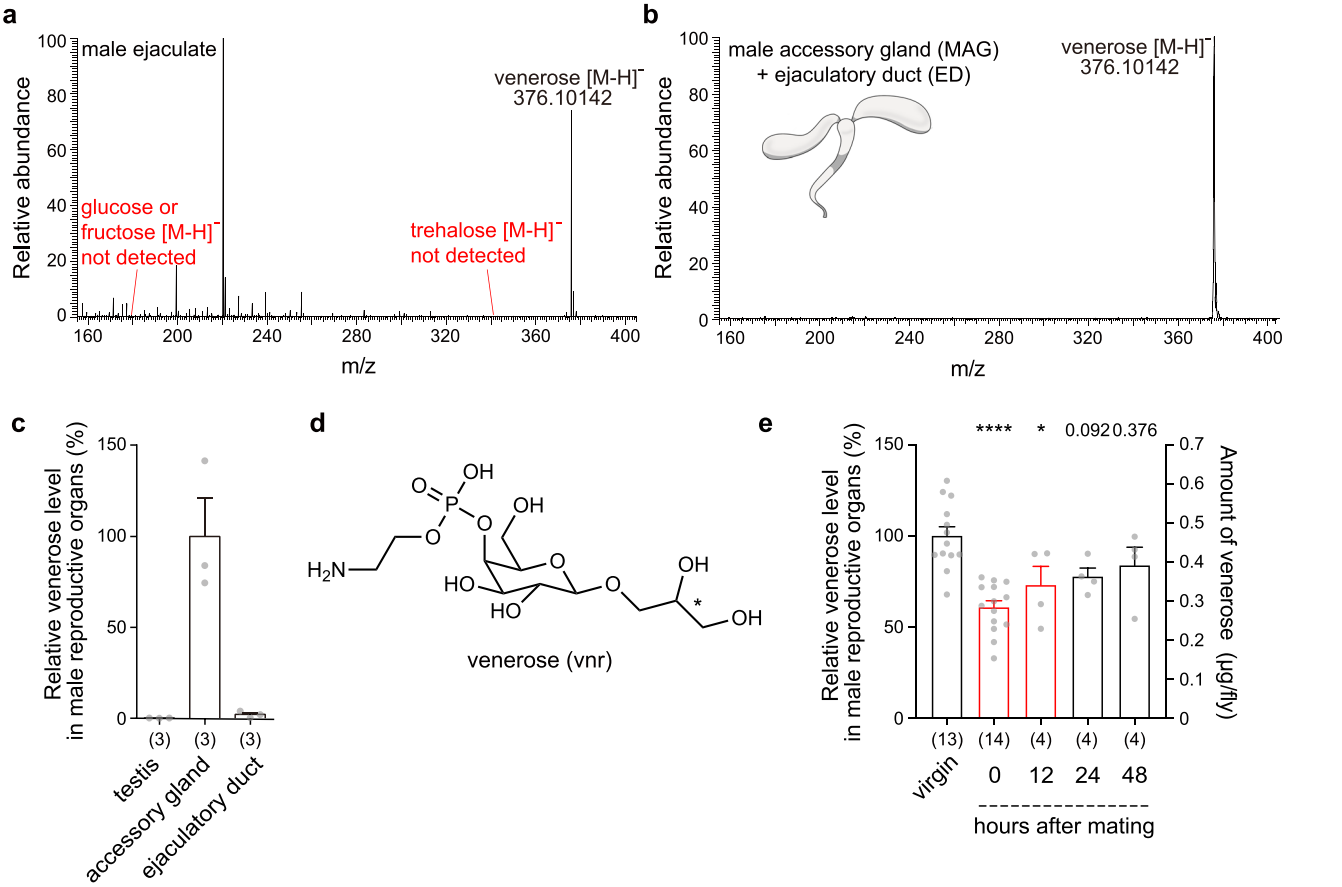

Fig. 1 | Identification of venerose, a sugar-like substance rich in male *Drosophila* ejaculate. a, **b** Liquid chromatography-mass spectrometry (LC-MS) profile of the C_{18} flow-through of male ejaculate (**a**) and MAG and ED extracts (**b**). **c**, **e** Relative venerose levels in the indicated reproductive organs isolated from wild type *Canton-S* (*CS*) males (**c**) and in all the reproductive organs of *CS* males harvested at the indicated times post-mating (**e**). All data are shown as means ± SEM. The numbers in parentheses indicate *n*. One-way ANOVA with Bonferroni post-hoc tests (*$p < 0.05$, ****$p < 0.0001$). Exact *p*-values are in Supplementary Data 4. **d** The structure of venerose, 1-*O*-[4-*O*-(2-aminoethylphosphate)-β-$_D$-galactopyranosyl]-x-glycerol. Carbon atom marked with asterisk is a stereocenter of glycerol moiety. Source data are provided as a Source Data file.

Females absorb venerose from the male ejaculate

Drosophila females incorporate phosphorus from the male ejaculate into both somatic tissues and developing oocytes[22]. Since venerose carrying its phosphoethanolamine moiety is highly abundant in the male ejaculate, we hypothesized that females absorb phosphorus from the ejaculate via venerose. We radio-labeled venerose by feeding newly emerged males ^{32}P-containing medium for 5 days. When we did the same with *UGT305A1* knockdown flies, we saw a roughly 40% reduction in venerose production and a corresponding 40% reduction in ^{32}P radioactivity in the hydrophilic eluents of MAG extracts, suggesting most ^{32}P radioactivity in the MAG extracts originates from labeled venerose (Fig. 2d). In contrast, *UGT305A1* knockdown did not affect the ^{32}P activity of venerose-deficient head extracts (Fig. 2e). When examined 24 h after mating, the ovaries of females mated with *UGT305A1* knockdown males also had approximately 40% less ^{32}P activity than those of females mated with control males (Fig. 2f). These findings strongly suggest mated females absorb elemental phosphorus by metabolizing infused venerose. Furthermore, we detected venerose in hemolymph collected from mated females, but not from virgin females (Fig. 2g, Supplementary Fig. 1c). Copulation in *D. melanogaster* induces physical damage to the female reproductive system, allowing components of the ejaculate to diffuse passively into the hemocoel[44] and providing a plausible route by which venerose enters the female hemolymph.

Venerose is essential for mating-induced GSC proliferation

To assess the role of venerose in female reproduction, we examined egg-laying activity in females mated with venerose-deficient *UGT305A1* knockdown males. In these females, cumulative egg-laying activity over a period of 7 days was reduced by 37–66% (Fig. 3a). Venerose deficiency in the male ejaculate did not, however, appear to affect sperm fertility or offspring viability (Supplementary Fig. 5a–c).

Females inseminated by venerose-deficient males began showing reduced egg-laying activity roughly three days post-mating (Fig. 3a). It is therefore possible that venerose affects mating-induced germline stem cell (GSC) proliferation, then influencing egg production 2–3 days post-mating[10]. Females mated with control males showed an increase in GSCs, whereas females mated with *UGT305A1* knockdown venerose-deficient males showed reduced GSC proliferation (Fig. 3b, c). This impairment was restored by injecting 0.8 nmol of synthetic venerose (Fig. 3d). Venerose injection into virgin females also stimulated GSC proliferation to the levels observed in mated females (Fig. 3e). This effect appeared to be dependent on the amount of injected venerose, with amounts as low as 0.16 nmol inducing GSC proliferation (Supplementary Fig. 5d). This amount corresponds to roughly 35% of the total venerose transmitted during mating (see Discussion). Mating-induced GSC proliferation is mediated by Decapentaplegic (Dpp), the fly counterpart of bone morphogenetic protein (BMP)[10,13–15,45,46]. Venerose injection into virgin females increased phosphorylated Mad (pMad) in GSCs, indicating Dpp activity (Fig. 3f).

https://doi.org/10.1038/s41467-024-52807-3

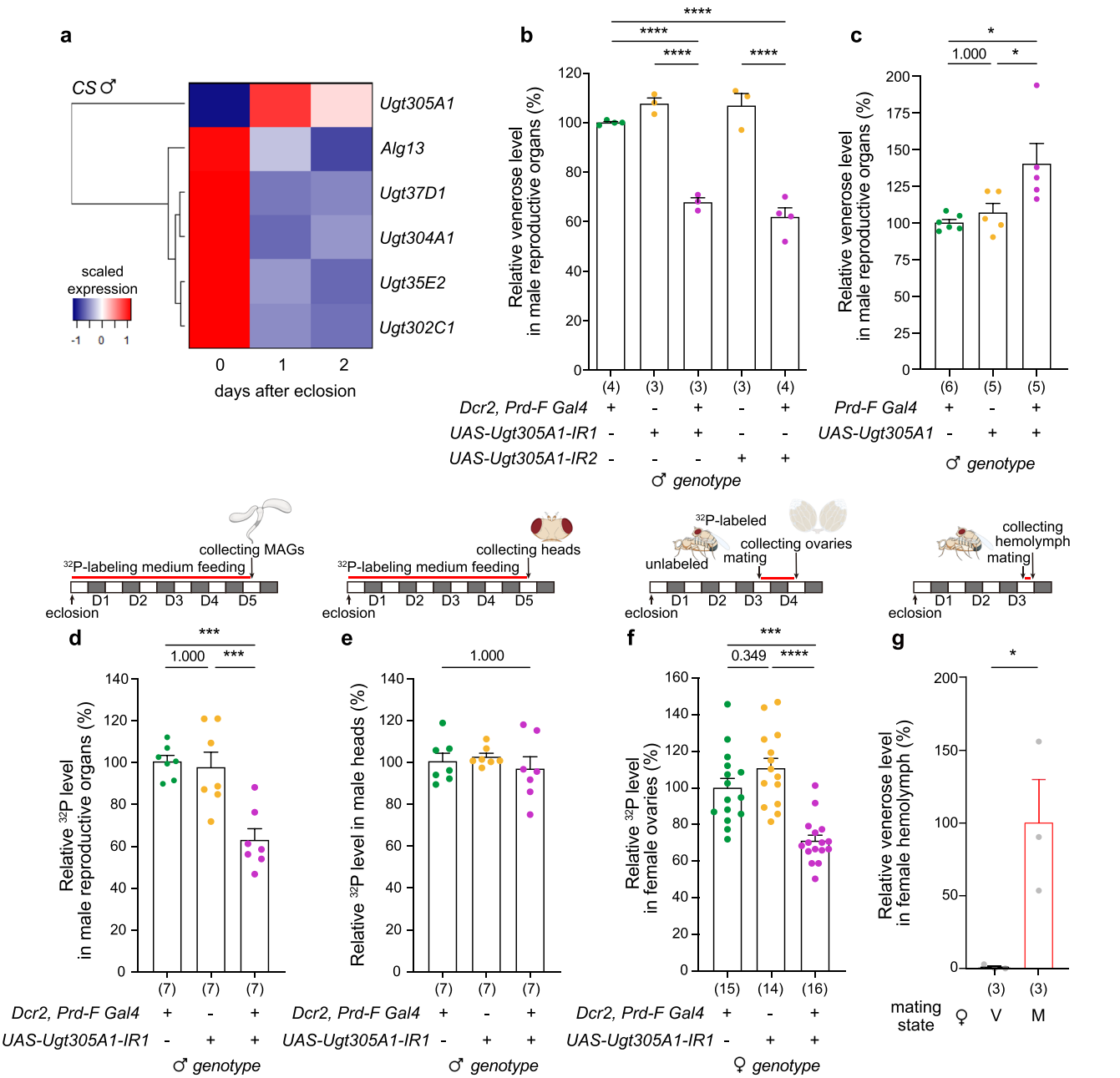

Fig. 2 | MAG-specific knockdown of the glycosyltransferase UGT305A1 inhibits venerose production and reduces phosphorus accumulation in the ovaries of females mated with knockdown males. a Heatmap representation (scaled expression) of the transcriptional changes at the indicated times post-eclosion for six GT28 genes expressed in the MAG. Count, tpm, and scaled values are available in Supplementary Data 2. **b**, **c**, **g** Relative venerose levels in male reproductive organs of the indicated genotypes (**b**, **c**) and in the hemolymph of virgin (V) or mated (M) females (**g**). Each dot represents a tissue sample from 5 flies (**b**, **c**) or a hemolymph sample from 10 flies (**g**). **d**–**f** Relative ^{32}P levels in the reproductive organs (**d**) and heads (**e**) of ^{32}P-labeled males of the indicated genotypes and in the ovaries of females mated with ^{32}P-labeled males of the indicated genotypes (**f**). Each dot represents a tissue sample from 3 flies. The schematics above the graphs illustrate the experimental protocol (**d**–**g**). Data are shown as means ± SEM. The numbers in parentheses indicate *n*. One-way ANOVA with Bonferroni post-hoc tests (**b**–**f**). Unpaired two-tailed *t*-tests (**g**). The numbers above the columns are *p*-values (*$p < 0.05$, ***$p < 0.001$, ****$p < 0.0001$). Exact *p*-values are in Supplementary Data 4. Source data are provided as a Source Data file.

Venerose stimulates GSC proliferation via a brain factor

Next, we asked whether venerose acts directly on the ovary to stimulate GSC proliferation. First, we isolated ovaries from virgin females and incubated them in culture medium supplemented with or without venerose. As a positive control, we used 1 mM octopamine (OA) to stimulate GSC proliferation to the level observed in mated females[14]. Unlike with OA, however, we found 10 mM venerose did not affect GSC numbers in cultured ovaries (Fig. 3g). We therefore formulated another hypothesis in which venerose acts indirectly via another tissue, such as the brain or gut, by triggering the release of an external factor(s) that stimulates GSC proliferation[10,15,47]. Indeed, we found significantly more GSCs in ovaries co-cultured with brains in medium supplemented with venerose, but not in medium without it (Fig. 3h). A similar co-culture with gut in venerose-containing medium, however, did not stimulate GSC proliferation (Fig. 3h). These observations suggest venerose acts on the brain to induce the secretion of an endocrine factor that then stimulates GSC proliferation in the ovaries.

https://doi.org/10.1038/s41467-024-52807-3

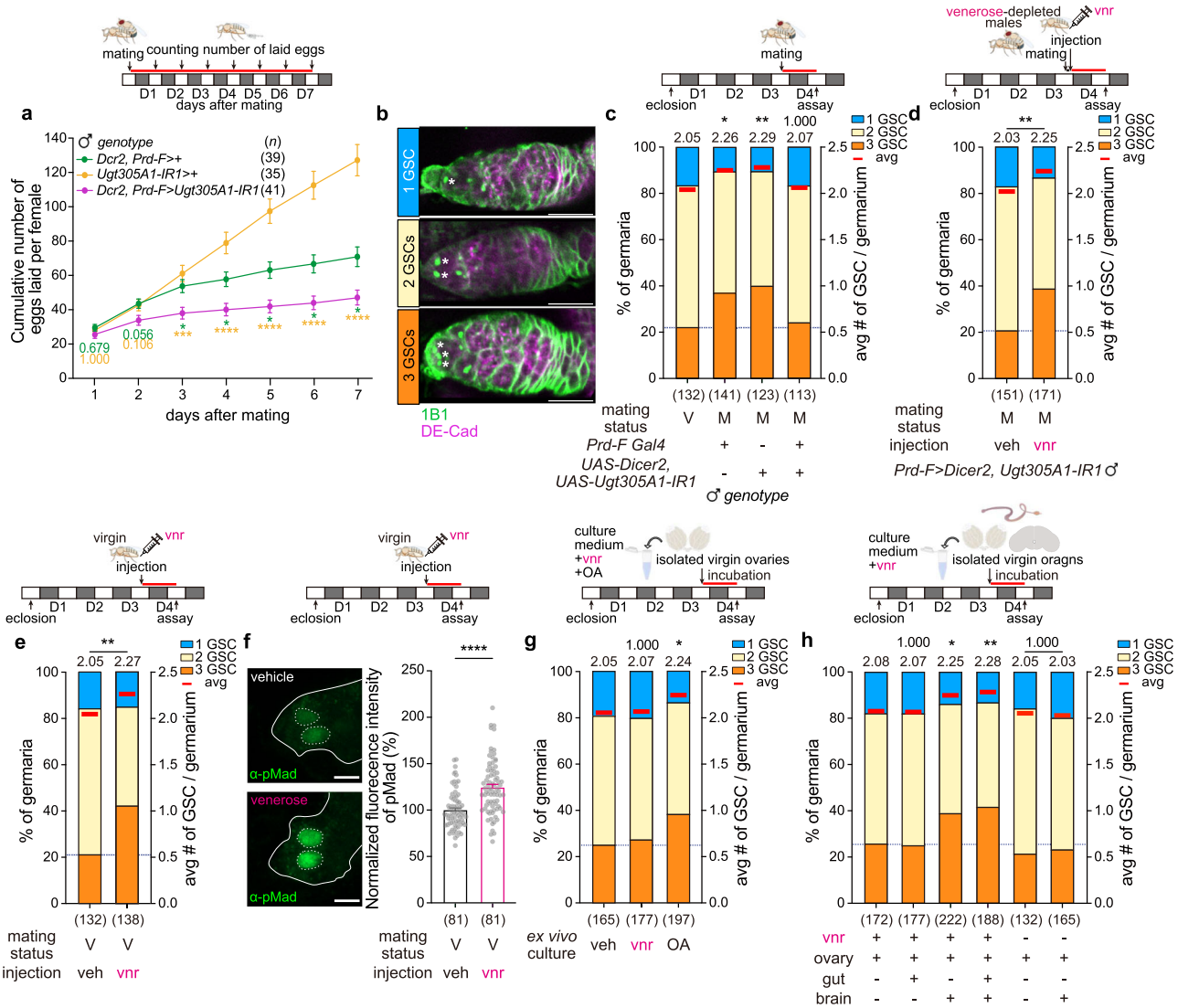

Fig. 3 | Venerose stimulates GSC proliferation via the brain. a Cumulative number of eggs laid per female mated with a male of the indicated genotypes. The *p*-value is color-coded by test groups. **b** Representative images of female adult germaria containing 1, 2, or 3 GSCs. The samples are immunostained with anti-1B1 (a GSC marker) and anti-DE-cadherin (a cell membrane marker). Asterisks indicate GSCs. **c**–**e**, **g**, **h** Frequencies of germaria containing 1, 2, or 3 GSCs (*left y-axis*) and the average number of GSCs per germarium (*right y-axis*). **c** Virgin females (V) or females mated with a male of the indicated genotypes. **d** Females received an injection of vehicle or 0.8 nmol of venerose 4 hours after mating with venerose-depleted males. Ovaries were examined 24 h post-injection. **e** Virgin females that received an injection of vehicle or venerose. **g** Virgin ovaries cultured for 24 h in a medium containing vehicle, 10 mM venerose, or 1 mM octopamine (OA). **h** Virgin ovaries cultured for 24 h in vehicle or 10 mM venerose along with gut or brain tissues from w^{1118} virgin females. Columns 5 and 6 are from a different experimental cohort. **f** Representative images of germaria from virgin females that received an injection of vehicle or venerose and stained with an anti-pMad (left). Normalized anti-pMad immunoactivity in GSCs from the injected females (right). The data are shown as means ± SEM. The schematics illustrate experimental protocol. The numbers in parentheses indicate *n*. The dotted lines represent the frequency of germaria with 3 GSCs in control conditions (*leftmost*). The numbers above the bars indicate the average number of GSCs per germarium. The numbers above the columns indicate the *p*-values (*$p < 0.05$, **$p < 0.01$). Exact *p*-values are in Supplementary Data 4. One-way ANOVA with Bonferroni post-hoc analysis (**a**). Kruskal-Wallis tests with Dunn post-hoc tests (**c**, **g**, **h**). Two-tailed Mann Whitney tests (**d**–**f**). Scale bars, 20 μm (**b**), 5 μm (**f**). Source data are provided as a Source Data file.

Dh44 acts on the ovaries to trigger GSC proliferation

Dh44-R2, one of two GPCR receptors sensitive to Dh44, is expressed in terminal filament (TF) cells in larval ovaries[48]. We verified its expression in TFs and discovered its expression in transition cells (TCs), which are TF cells that contact cap cells in the adult ovary (Fig. 4a–d, Supplementary Fig. 6a–d). TF cells, cap cells, and escort cells comprise the GSC niche, which provides a physical anchor for GSCs and controls their maintenance and proliferation[49,50]. Dh44-R1, a paralogue of Dh44-R2, does not appear to be expressed in GSC niche cells or other ovarian cells (Supplementary Fig. 6c). The expression of Dh44-R2 in GSC niche cells suggests that its ligand Dh44, which is secreted by the brain in response to circulating venerose, may be involved in mating-induced GSC proliferation. We cultured virgin ovaries in medium containing varying concentrations of Dh44 and found that levels of synthetic Dh44 as low as 10 nM stimulate GSC proliferation as much as 1 mM OA (Fig. 4e). Next, we wanted to investigate the role of TF cell Dh44-R2 in Dh44-induced GSC proliferation. Although bab1-Gal4 is commonly used to target transgenes to TF cells, we realized it is also expressed outside the ovary, such as in cells of the brain and gut[51]. Thus, we compared the expression of bab1-Gal4 and Dh44-R2 and found that their ovarian expression overlapped only in TF cells of the germarium (Supplementary Fig 6e–j). To avoid any compounding effect due to unknown overlap of bab1-Gal4 and Dh44-R2 expression in other tissues, we performed ex vivo culture

https://doi.org/10.1038/s41467-024-52807-3

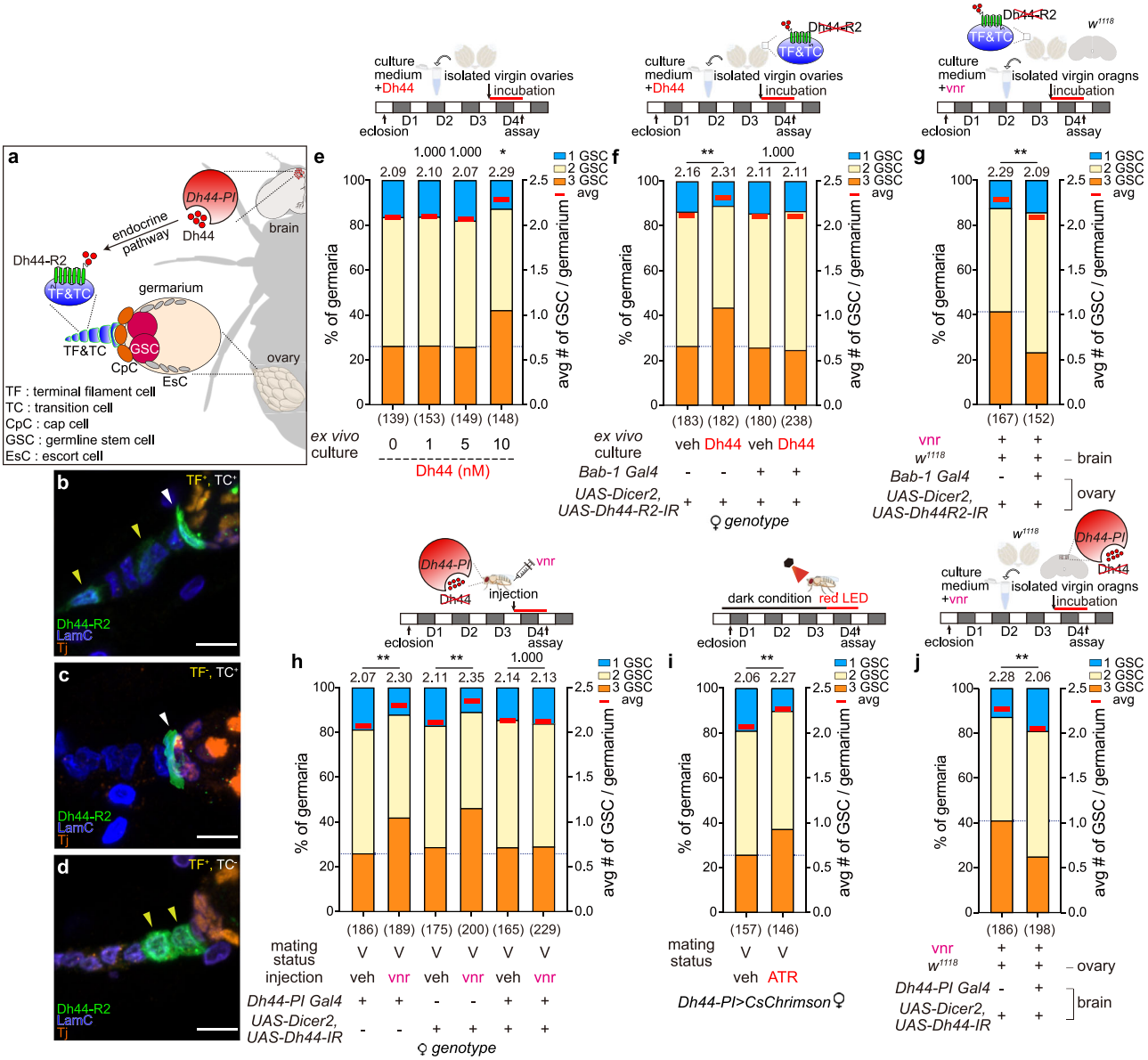

Fig. 4 | The neuropeptide Dh44, secreted by brain Dh44-PI neurons, and its receptor Dh44-R2, expressed in GSC niche cells, are essential for venerose-induced GSC proliferation. a A schematic illustrating inter-organ signaling between the brain and the ovary, where Dh44, secreted into the hemolymph by Dh44-PI neurons, stimulates GSC proliferation through its receptor expressed in the TF cells of the GSC niche. **b**-**d** Representative confocal Z-projection images of germaria from *Dh44-R2 > mCD8-EGFP* females immunostained with anti-GFP, anti-LamC (a GSC niche cell marker), and anti-Tj (a cap cell marker) ($n = 24$). All examined germaria exhibited one of three types of Dh44-R2 expression in TF and TC cells at the following frequencies: TF + TC + 54% (**b**), TF- TC + 38% (**c**), TF + TC- 8% (**d**). TF and TC cells are indicated by yellow and white arrow heads, respectively. Scale bars, 5 μm. **e**–**j** Frequencies of germaria containing 1, 2, or 3 GSCs (*left y-axis*) and the average number of GSCs per germarium (*right y-axis*). **e** Virgin ovaries of w^{1118} cultured for 24 h in a medium containing Dh44 at the indicated concentrations. **f** Virgin ovaries of the indicated genotypes and cultured for 24 h with or without 10 nM Dh44. **g** Virgin ovaries of the indicated genotypes and cultured for 24 h in 10 mM venerose along with female virgin w^{1118} brains. **h** Ovaries from virgin females of the indicated genotypes that received an injection of vehicle or 0.8 nmol venerose. Ovaries were examined 24 h post-injection. **i** Ovaries isolated from virgin females exposed to 24 h of light activation. Females were fed vehicle or all-*trans*-retinal (ATR) immediately after eclosion. **j** Virgin ovaries of w^{1118} cultured for 24 h in 10 mM venerose along with virgin female brains of the indicated genotypes. The schematics illustrate the experimental protocols. The numbers in parentheses indicate *n*. The numbers above the columns indicate the *p*-values for the indicated comparisons (*$p < 0.05$, **$p < 0.01$). Exact *p*-values are in Supplementary Data 4. Kruskal-Wallis tests with Dunn post-hoc tests (**e**, **f**, **h**). Two-tailed Mann Whitney tests (**g**, **i**, **j**). Source data are provided as a Source Data file.

experiments using ovaries isolated from bab1-Gal4-induced *Dh44-R2* knockdown and observed a complete inhibition of Dh44-induced GSC proliferation (Fig. 4f). This suggests a direct mode of action for Dh44 on the ovary. Moreover, when we co-cultured *Dh44-R2* knockdown ovaries with brains in venerose-containing medium, they showed no obvious signs of GSC proliferation, unlike control ovaries (Fig. 4g). We were also able to corroborate these observations with in vivo experiments using mated females. *Dh44-R2* knockdown prevented the increase in GSC proliferation and pMad activity we observed in control females (Supplementary Fig. 7a, b). In contrast, *Dh44-R1* deficiency had no effect on Dh44-induced GSC proliferation (Supplementary Fig. 7c, d). From these results, we conclude that after entering the female's hemolymph from the male ejaculate, venerose stimulates $Dh44^+$ neurons in the brain to secrete Dh44. This Dh44 then acts on GSC niche cells expressing Dh44-R2 to promote GSC proliferation (Fig. 4a).

Venerose stimulates GSC proliferation via Dh44-PI neurons

Many brain neurons express Dh44, but the 6 endocrine Dh44-expressing Dh44-PI neurons in the *pars intercerebralis* express the highest levels of Dh44[31]. Dh44-PI neurons secrete Dh44 in response to hemolymph-born sugars[35,36]. We therefore hypothesized that Dh44-PI neurons may also secrete Dh44 in response to venerose, subsequently stimulating GSC proliferation. When we injected venerose into *Dh44-RNAi* virgin females whose Dh44-PI neurons no longer produce Dh44, they did not show the venerose-induced increase in GSCs observed in controls (Fig. 4h). Next, we activated Dh44-PI neurons with the light-sensitive cation channel *CsChrimson*, which requires all-trans-retinal (ATR) for activation. After 24 h of light exposure, females fed an ATR-containing diet but not those fed an ATR-free diet showed enhanced GSC proliferation (Fig. 4i). We also performed ex vivo culture experiments to validate the necessity of Dh44 secreted by Dh44-PI neurons. Virgin ovaries co-cultured with control brains but not *Dh44* knockdown brains showed a significant increase in GSCs in response to venerose (Fig. 4j).

Venerose stimulates Dh44-PI neurons to secrete Dh44

Thus far, our results indicate that venerose enters the female hemolymph after mating. Because males transfer ~40% of the contents of their MAG in a single mating session (Fig. 1e) and because MAG extracts from individual males contain ~1.2 nmol of venerose, we estimate that venerose levels could reach 6 mM in the female hemolymph. Consistent with this estimate, we found that treatment of isolated brains with as low as 2 mM synthetic venerose induced a significant decrease in Dh44 protein levels in Dh44-PI neurons. This indicates that venerose induces Dh44 secretion at physiologically relevant concentrations (Fig. 5a). To further examine the role venerose plays in Dh44 secretion, we asked whether venerose can trigger Ca^{2+} oscillations in Dh44-PI neurons expressing the Ca^{2+} reporter GCaMP6m. In brain preparations containing tetrodotoxin (TTX) to eliminate any synaptic input on the Dh44-PI neurons, we found the addition of 2 mM synthetic venerose induced a Ca^{2+} response in ~40% of Dh44-PI (Fig. 5b–d). Venerose produced longer-lasting Ca^{2+} dynamics than glucose (Fig. 5b, Supplementary Movie 1), with an oscillation duration of 128 ± 45 s (for 2 mM). Notably, 2 mM venerose stimulated robust Ca^{2+} oscillations in Dh44-PI neurons with a latency of 8.3 ± 1.4 min. In a copulation episode lasting ~15 min, ejaculate transfer is completed within 7–8 minutes of copulation initiation[52]. This suggests the Dh44-PI neurons begin Dh44 secretion roughly by the end of copulation.

Venerose stimulates Dh44-PI neurons via Tret1-1

Dh44-PI neurons regulate post-ingestive nutrient selection, with Ca^{2+} oscillations in response to nutritive D-glucose, but not to non-nutritive L-glucose[35]. Since the sugar transporter blocker phlorizin can suppress nutritive sugar-induced Ca^{2+} oscillations[35], we reasoned that sugar transporters in Dh44-PI critical for post-ingestive nutrient selection may also be important for responsiveness to venerose. After knocking down 23 *Drosophila* sugar transporters in Dh44-PI neurons, we found that knockdown of *trehalose transporter 1-1 (Tret 1-1)* impaired D-glucose selection and reduced D-glucose-induced Ca^{2+} oscillations (Supplementary Fig. 8; Fig. 5e). Furthermore, *Tret1-1* knockdown significantly reduced venerose-induced Ca^{2+} oscillations, Dh44 secretion, and GSC proliferation (Fig. 5e–g).

Energy-deprived females absorb more venerose

Males transfer considerable amounts of venerose to females during mating. The elemental phosphorus females absorb from the male ejaculate is predominantly derived from venerose (Fig. 2g). This suggests venerose transfer may function as a form of seminal feeding, akin to courtship feeding. To further explore this, we investigated the relationship between female energy state and absorption of venerose. When mated with males producing ^{32}P-labelled venerose, the ovaries of starved females exhibited higher ^{32}P activity than their well-nourished counterparts (Fig. 6a), indicating that energy-deprived conditions lead to increased female venerose absorption. As females can only absorb venerose while retaining the male ejaculate in their uterus, energy states that enhance venerose absorption likely extend the EHP.

Energy-dependent effects of venerose on EHP and sperm storage

Given the essential role of Dh44 from Dh44-PI neurons in establishing the standard EHP (~90 min) and facilitating adequate sperm storage[31], our finding that venerose stimulates Dh44 secretion suggests a potential regulatory role for venerose in EHP and sperm storage dynamics. Dh44-PI neurons function as nutrient sensors, particularly during energy-deprived states[36], indicating heightened responsiveness to venerose under starved conditions. Starved females, when mated with control males, exhibited significantly longer EHP durations than their well-nourished counterparts (Fig. 6b). But pairings with *UGT305A1* knockdown males, which produce ~40% less venerose than control males, resulted in markedly shorter EHPs and reduced sperm storage (Fig. 6b, c). Importantly, this effect was exclusive to starved females; we did not observe any notable effect in their well-nourished counterparts. These results suggest venerose transferred by males induces energy-deprived females, but not well-nourished ones, to extend their EHP, leading to enhanced venerose absorption and sperm storage.

Energy state determines Dh44 pool size

When we monitored Ca^{2+} oscillations in Dh44-PI through a small window on the head capsule of live flies, well-nourished females produced spontaneous oscillations with larger amplitudes than starved females (Supplementary Fig. 9a). Thus, well-nourished females secrete more Dh44 peptide, leaving less in the Dh44-PI neurons. We corroborated this finding when we observed a significant increase in anti-Dh44 immunoreactivity in Dh44-PI neurons under starvation conditions (Fig. 6d). Next, we further investigated the relationship between Dh44-PI activity, Dh44 pool, and EHP. Optogenetic inhibition of Dh44-PI neurons before mating increased Dh44 peptide levels by 67 ± 21.3% and EHP by 24 min compared to controls (Fig. 6e), while thermal activation of Dh44-PI neurons reduced Dh44 peptide levels by 42 ± 9.6% and EHP by 56 minutes (Fig. 6f). These results suggest increased Dh44-PI activity and reduced Dh44 levels before mating reduce the EHP of female flies, whereas decreased Dh44-PI activity and elevated Dh44 levels prolong the EHP.

We observed a marked reduction in Dh44 peptide levels in mated females compared to virgins, regardless of their energy state prior to mating (Supplementary Fig. 9b, c). This indicates that mating and venerose stimulate Dh44-PI neurons to secrete large amounts of Dh44. We infer from these results that the energy state of females before mating determines the size of the Dh44 pool available for secretion triggered by mating or venerose (Fig. 6g). Under well-nourished conditions, Dh44-PI neurons have a limited Dh44 pool because of their high level of spontaneous activity, probably induced by elevated hemolymph sugars. Conversely, under energy-deprived conditions, Dh44-PI neurons possess a much larger Dh44 pool. Consequently, when mated with control males that transfer a substantial amount of venerose, energy-deprived females with larger Dh44 pools secrete more Dh44, exhibit extended EHP, and absorb a greater amount of venerose compared to well-nourished females with limited Dh44 pools.

Females assess the energy status of male partners via venerose

Males under low-energy conditions produce and allocate less nutrients in their ejaculate[53]. We found that males starved for 24 h

https://doi.org/10.1038/s41467-024-52807-3

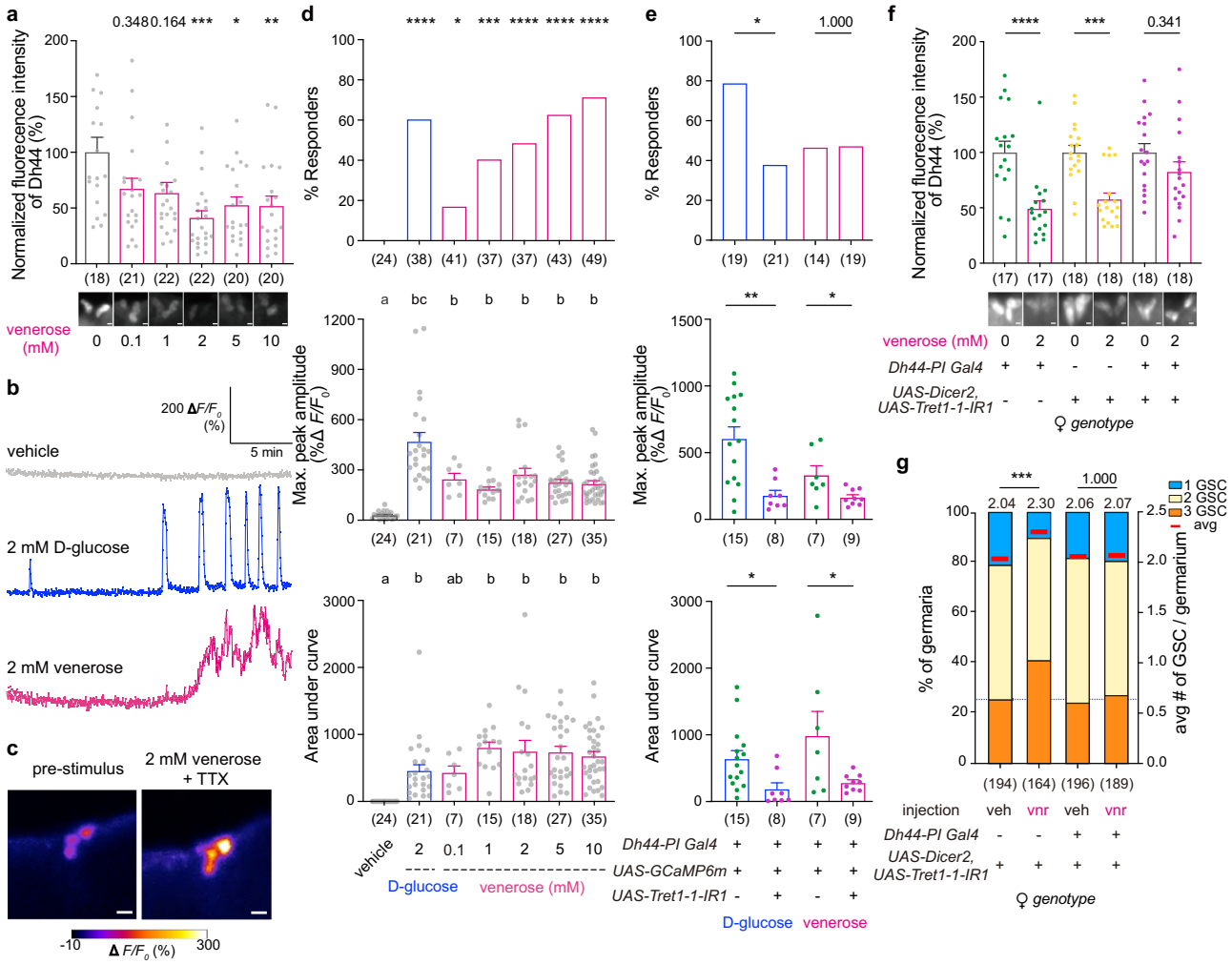

Fig. 5 | Venerose stimulates Ca^{2+} transients and Dh44 secretion in Dh44-PI neurons via the sugar transporter Tret1-1. a, **f** Normalized anti-Dh44 immunoreactivity in Dh44-PI neurons from virgin females of the indicated genotypes stained with anti-Dh44 antibody after a 30-min treatment with venerose at the indicated concentrations. The immunoreactivity of each soma was quantified. Dots indicate normalized anti-Dh44 fluorescence intensity from individual females. The data are shown as means ± SEM. Scale bars, 5 μm. **b** Representative GCaMP fluorescence traces of Dh44-PI neurons immediately after applying the indicated substances. **c** Representative GCaMP fluorescence images from Dh44-PI neurons 20 min after applying the indicated substances ($n = 18$). Scale bars, 10 μm. **d**, **e** GCaMP fluorescence responses of Dh44-PI neurons from virgin females of the indicated genotypes to D-glucose or venerose at the indicated concentrations (**d**) or to 2 mM D-glucose or 2 mM venerose (**e**). For % responders (*above*), data are shown as means. For the maximum peak amplitude (*middle*) and area under curve (*below*), data are shown as means ± SEM. The numbers in parentheses indicate *n*. Two-sided Fisher's exact tests comparing vehicle control with the indicated treatments (**d**, **e**, *above*). One-way ANOVA with Bonferroni post-hoc tests (**d**, *below*; **f**) and Kruskal-Wallis tests with Dunn post-hoc tests comparing vehicle control with venerose treatment at the indicated concentrations (A and D *middle*). Unpaired two-tailed *t*-tests (**e**, *middle* and *below*). The letters above the columns in (**d**) indicate significant differences ($p < 0.05$) for comparisons of each treatment. The numbers above the columns are *p*-values (*$p < 0.05$, **$p < 0.01$, ***$p < 0.001$, ****$p < 0.0001$). Exact *p*-values are in Supplementary Data 4. **g** Frequencies of germaria containing 1, 2, or 3 GSCs (*left y-axis*) and the average number of GSCs per germarium (*right y-axis*) from the ovaries of virgin females of the indicated genotypes that received an injection of vehicle or 0.8 nmol venerose. The numbers above the columns indicate the *p*-values for the indicated comparisons. Kruskal-Wallis tests with Dunn post-hoc tests. Source data are provided as a Source Data file.

produced only half the venerose of well-nourished males (Fig. 7a). In contrast to venerose, starvation had a limited effect on SP levels (Fig. 7b). This suggests a male's energy state has a greater effect on seminal fluid venerose levels than SP levels. Moreover, females mated with starved males exhibited no signs of mating-induced GSC proliferation (Fig. 7c).

Last, since male energy status influences seminal fluid venerose levels, we asked whether females adjust EHP and sperm storage in response to the energy state of their male partners. As anticipated, we found starved females mated with males starved for 24 h exhibited an EHP 23 minutes shorter than those mated with well-nourished males and stored 19.4% less sperm (Fig. 7d, e). In contrast, well-nourished females did not exhibit any discernible changes in EHP or sperm storage when exposed to the seminal fluid of starved males.

Together, these findings provide insight into a mechanism by which females, particularly those malnourished prior to mating, can discern males with distinct energy states by adjusting EHP and sperm storage (Fig. 7f). In energy-deprived conditions, females possess a larger Dh44 pool. In this situation, as the quantity of venerose in seminal fluid increases, Dh44 secretion increases, leading to increased EHP and consequently enhanced sperm storage. Well-nourished females, in contrast, have limited a Dh44 pool that is easily depleted by the smaller amounts of venerose transferred by starved males. For these females, Dh44 secretion cannot increase further in response to the seminal fluid of well-nourished males, which leads to a resistance to changes in the EHP and sperm storage regardless of variations in the quantity of venerose transferred by males.

https://doi.org/10.1038/s41467-024-52807-3

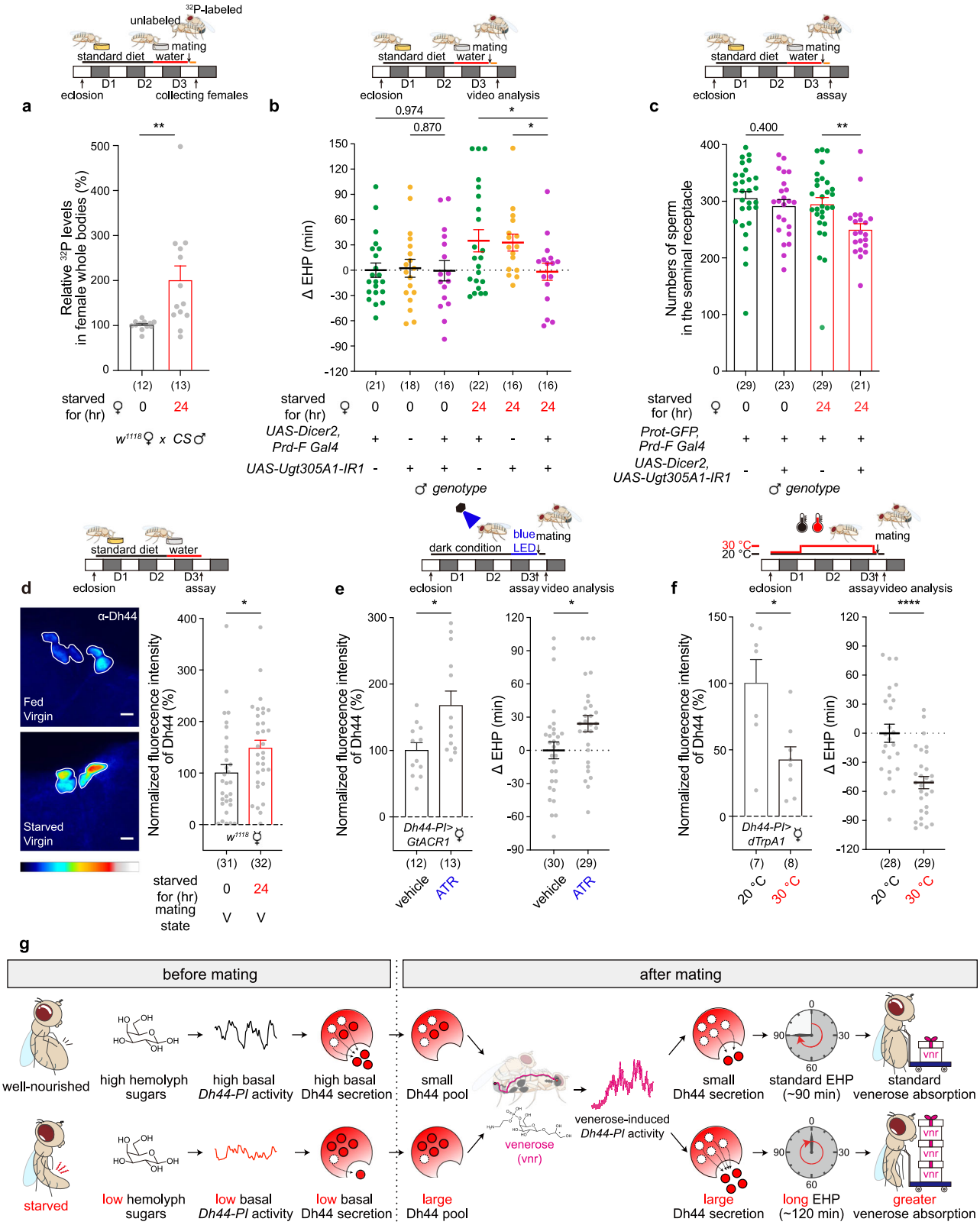

Discussion

Venerose is a signaling molecule that activates the Dh44 system during mating

In this study, we identified venerose as a signaling molecule that stimulates Dh44-PI neurons to release Dh44, which then affects GSC proliferation and modulates EHP and sperm storage. Multiple findings suggest venerose enters the female hemolymph and activates the Dh44 system during mating. First, although venerose is normally produced exclusively in the MAG along with seminal fluid, it was detected in female hemolymph post-mating. Second, females mated to males producing low venerose levels exhibited virgin-like GSC proliferation levels that were restored by venerose injection. Third,

Fig. 6 | Nutritional stress in females extends EHP duration and enhances venerose absorption by increasing the Dh44 pool available for venerose-induced secretion. a Relative ^{32}P levels in whole female bodies of females under the indicated feeding conditions before mating with ^{32}P-labeled *CS* males. Females were examined 4 h post-mating, by which time all females had completed expulsion of the male ejaculate. Each dot represents the relative ^{32}P level of a tissue sample from 3 flies. **b** Normalized EHP (ΔEHP) from w^{1118} females under the indicated feeding conditions before mating with a male of the indicated genotypes. The EHP was normalized by subtracting the EHP from females under the indicated conditions by the mean of the reference EHPs (*leftmost column*). **c** Number of sperm stored in the seminal receptacles of well-nourished or starved females before mating with a male of the indicated genotypes. **d** Heatmap images (*left*) and normalized anti-Dh44 immunoreactivity of Dh44-PI neurons from w^{1118} females of the indicated nutritional and mating status stained with anti-Dh44 antibody. Increasing Dh44 levels are indicated by blue, green, yellow, and red, in order. Quantified immunoreactivity of somas (outlined in white in the left panel). V indicates virgin females. Circles indicate the normalized anti-Dh44 fluorescence intensities from individual females. Scale bars, 10 μm. Images are Z-projections with averaged intensity. **e**, **f** Left, normalized anti-Dh44 immunoreactivity from virgin females of the indicated genotypes stained with anti-Dh44 antibody. Quantified soma immunoreactivity. Circles indicate the normalized anti-Dh44 fluorescence intensity of individual females. Right, normalized EHP (ΔEHP) from females under the indicated conditions mated with *CS* males. Circles indicate ΔEHP measured from individual females. ATR indicates females fed all-trans-retinal. The schematics above the graphs illustrate each experimental protocol. Data are shown as means ± SEM. The numbers in parentheses indicate *n*. One-way ANOVA with Bonferroni post-hoc analysis (**b**, **c**). Unpaired two-tailed *t*-tests (**a**, **d**–**f**). The numbers above the columns are *p*-values ($^{*}p < 0.05$, $^{**}p < 0.01$, $^{****}p < 0.0001$). Exact *p*-values are in Supplementary Data 4. Source data are provided as a Source Data file. **g** A model explaining energy-state dependent EHP extension and venerose absorption (see Result).

control virgins injected with venerose exhibited mated-female-like GSC proliferation, but females with Dh44-PI neurons unable to produce Dh44 were unresponsive to venerose. Fourth, ovaries co-cultured with functional Dh44-PI neurons increased GSC proliferation in response to venerose. Last, 2 mM venerose induced robust Ca^{2+} responses in an ex vivo calcium imaging preparation, leading to increased Dh44 secretion. Males transfer roughly 40% of the venerose pool in the MAG (0.48 nmol) during mating and females have roughly 80 nl of hemolymph volume[54]. Thus, assuming a conservative 35% absorption rate, mating could produce venerose levels in the female hemolymph of up to 2 mM. This aligns precisely with the estimates we gleaned from our venerose injection experiments.

Dh44 regulates GSC proliferation and EHP expansion via distinct GPCR pathways

Our findings indicate that Dh44-R2, expressed in GSC niche TC and TF cells, is essential for stimulating GSC proliferation in response to Dh44. In contrast to GSC proliferation, EHP is regulated by another Dh44 receptor, Dh44-R1 expressed in the CNS neurons. Thus, GSC proliferation and EHP expansion, which are regulated by different Dh44 receptors, will be regulated by different levels of Dh44 and therefore venerose.

Our data showed that females starved for 24 h absorbed almost twice as much venerose as well-fed females. Thus, we expected starved females would secrete more Dh44, prolonging EHP and increasing GSC proliferation. Contrary to our expectations, we found that females starved for 24 h before mating, despite exhibiting an EHP approximately 30 min longer, did not have higher GSC levels than well-fed females after mating with a well-nourished male (compare the second column of Fig. 7c with the third column of Supplementary Fig. 10a). This is probably because GSC proliferation peaks at lower levels of venerose and lower levels of Dh44 than EHP expansion. In addition, virgin females starved for 24 hours did not appear to show any noticeable difference in GSCs compared to their well-nourished counterparts (Supplementary Fig. 10a).

Venerose, a non-protein seminal substance that promotes GSC proliferation

Mating induces dramatic changes in female reproductive behavior and physiology, enhancing reproductive output[55–57]. In fruit flies, many of these mating-induced changes are elicited by the seminal fluid protein SP. In contrast to SP, which acts through 20E, OA, and NPF originating from peripheral organs, venerose operates through the Dh44 system within the brain. While OA and NPF signal through escort cells, Dh44 acts through TF cells, which have direct contact with cap cells. Despite these factors acting through distinct GSC niche cells, they all seem to play essential roles in enhancing Dpp activity in the GSCs of mated females[10,14,15] (and this study). Furthermore, we found that synthetic venerose induces normal levels of GSC proliferation even in virgin females lacking *Oamb*, which encodes the OA receptor essential for OA-induced GSC proliferation in mated females (Supplementary Fig. 10b). This suggests that either venerose or Dh44 acts independently of the OA signaling pathway. Thus, we postulate that mating-induced GSC proliferation requires both venerose-induced TF and TC signals and SP- or OA-induced escort cell signals to converge on the niche cap cells that produce Dpp—the major niche-derived stemness factor for GSC maintenance and proliferation.

Venerose transfer is a form of courtship feeding signaling male quality

In *D. melanogaster*, males engage in seminal feeding, a form of courtship feeding that allows females to incorporate male-derived phosphorus into their ovarian oocytes[22]. Until now, the specific source of the phosphorus acquired via seminal feeding remained elusive. Using ^{32}P-labeling experiments with *UGT305A1* knockdown males, we argue that most of the phosphorus absorbed by females during a mating episode is derived from venerose. Two findings support this claim. First, phosphorus NMR analysis of hydrophilic MAG extracts identified venerose as the single major source of phosphorus. Second, *UGT305A1* knockdown reduced total venerose in MAG extracts by approximately 40% (Fig. 2b). This roughly corresponds to the reduction in phosphorus-containing material in MAG extracts of *UGT305A1* knockdown males, as well as the reduction in phosphorus absorbed by females mated to *UGT305A* knockdown males (Fig. 2d, f). Although these observations do not completely rule out the possibility that *UGT305A1* knockdown affects the production of other phosphorus-containing seminal substances, the hypothesis that venerose serves as a nutrient source for females to absorb elemental phosphorus, a crucial nucleic acid component required for egg production, remains valid. Nevertheless, a comparison of phosphorus contained in a holidic medium[58] for *D. melanogaster* (6.8 ng/nl) with phosphorus females obtain in a single mating episode (~5.2 ng) suggests females obtain most of their phosphorus from their diet, at least under laboratory conditions.

In general, courtship feeding conveys information about male attractiveness or quality, making it common for females to prefer gift-giving males[24,25,59]. There is also a clear link between courtship feeding and post-mating sexual selection[26,27]. Venerose seems to influence two crucial aspects of female reproduction with significant implications for sexual selection: oogenesis and sperm storage. Therefore, the transmission of venerose can be considered a manifestation of courtship feeding that effectively communicates male quality and enhances reproductive success for the male donor.

Nutritional stress enhances acceptance of courtship feeding

The energy-state dependent acceptance of courtship feeding and sexual selection has been reported in many species[28,60]. For instance, in

https://doi.org/10.1038/s41467-024-52807-3

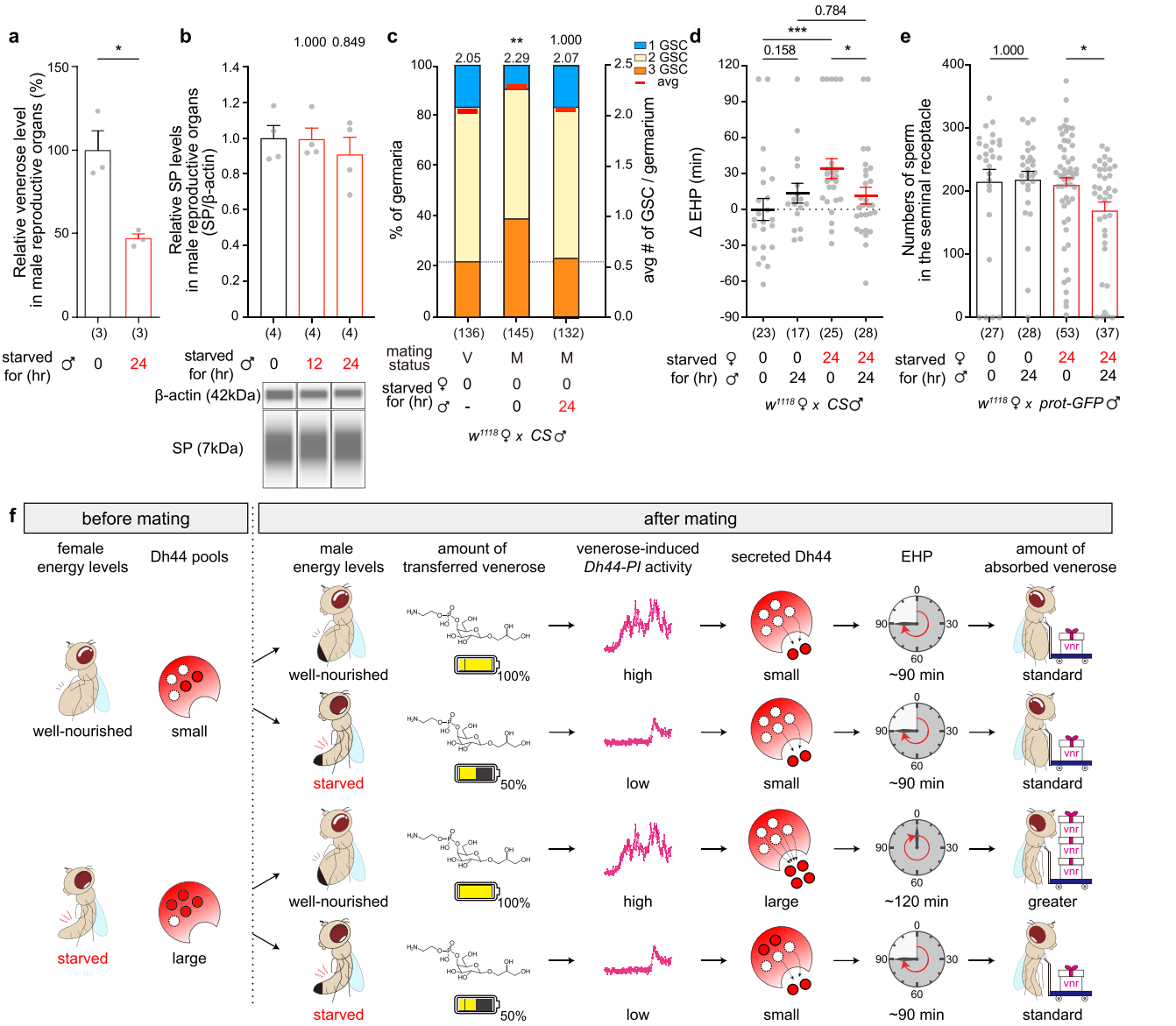

Fig. 7 | Under nutritional stress conditions, females discern the energy states of their mates by extending EHP, absorbing more venerose, and storing a greater amount of sperm from well-nourished males compared to undernourished males. a Relative venerose levels in the reproductive organs of *CS* males under the indicated feeding conditions. **b** Relative SP levels in the reproductive organs of *CS* males under the indicated conditions. The gel images below show representative Western data of β-actin (loading control) and SP proteins. **c** Frequencies of germaria containing 1, 2, or 3 GSCs (*left y-axis*) and the average number of GSCs per germarium (*right y-axis*) from virgin ovaries (V) or ovaries from females mated (M) with a male of the indicated conditions. **d** Normalized EHP (ΔEHP) from w^{1118} females under the indicated conditions before mating with a male of the indicated conditions. EHPs were normalized by subtracting the EHPs from females under the indicated conditions by the mean of reference EHPs (*leftmost*). **e** The number of sperm stored in the seminal receptacles of well-nourished or starved females after mating with a *protamine-GFP* male under the indicated feeding conditions. Data are shown as means ± SEM. The numbers in parentheses indicate *n*. Unpaired two-tailed *t*-tests (**a**), Kruskal-Wallis tests with Dunn post-hoc tests (**c**), and one-way ANOVA with Bonferroni post-hoc analysis (**b**, **d**, **e**). The numbers above the columns are *p*-values (*$p < 0.05$, **$p < 0.01$, ***$p < 0.001$). Exact *p*-values are in Supplementary Data 4. A two-way ANOVA detected an interaction between sex and nutritional status in (**d**); $p = 0.0336$, (**e**); $p = 0.1432$. Source data are provided as a Source Data file. **f** A model explaining how females under nutritional stress sense the energy levels of their mating partners and modulate EHP and venerose absorption. Starved females have larger Dh44 pools that can sustain the increased Dh44 secretion induced by the larger venerose injections of well-nourished males. Thus, nutritionally stressed females increase Dh44 secretion and extend EHP more readily when they mate with well-nourished males. The prolonged EHP in starved females mated with well-nourished males results in increased venerose absorption.

D. subobscura, where males regurgitate food to feed females during courtship, starved females show a preference for mating with food-giving males over non-giving males, whereas well-nourished females do not discriminate[24]. Here, we revealed that starved *D. melanogaster* females retained ejaculate containing larger amounts of venerose longer in their uterus, absorbing more venerose and storing more sperm. Their well-nourished counterparts, however, did not exhibit as much retention of high-venerose ejaculate. Moreover, this phenomenon did not occur when females were mated with males producing significantly lower levels of venerose due to starvation or *UGT305A1* knockdown.

The Dh44 system couples oogenesis with energy state

For fruit flies in their natural habitat, feeding and mating are intimately associated, as mates encounter one another more frequently near patches of food[61]. Dh44-PI neurons, serving as nutrient sensors,

stimulate feeding through their downstream effectors[35,36]. Our finding that enhanced Dh44-PI activity also affects GSC proliferation suggests the Dh44 system links feeding and oogenesis. Thus, it is plausible that venerose-induced Dh44 secretion during mating could contribute to the increased appetite of mated females, along with their increased GSC proliferation. This post-mating increase in feeding may, in turn, sustain increased GSC proliferation by further augmenting Dh44 secretion, even after venerose clearance.

In certain species, males transfer a spermatophore containing both spermatozoa and nourishment, which females often consume after the completion of spermatozoa transfer[62–64]. In other species, males offer their own body parts as food for their mates[19,20]. Thus, the Dh44 system may also have evolved to enable females to regulate oogenesis in response to nuptial food gifts provided before or after mating.

A potential implication in mammalian systems

Certain genes encoding the seminal fluid proteins of *D. melanogaster* have undergone rapid evolution to the extent that no detectable orthologs are present in other *Drosophila* species[65–67]. Similarly, there is limited evidence supporting the existence of venerose outside of the *Drosophila* genus. In contrast, the *Drosophila* Dh44 peptide and its receptors exhibit sequence homology with the corticotropin releasing hormone (CRH) peptide and its receptors in mammals, suggesting conserved functions[35,68]. In mammals, CRH inhibits gonadotropin-releasing hormone (GnRH) secretion in the hypothalamus, ultimately resulting in amenorrhea and infertility[69,70]. Unlike these inhibitory functions on female reproduction in mammals, our findings here highlight the role of Dh44 in promoting female fruit fly reproduction. It is noteworthy that CRH expressed in the uterus contributes to embryo implantation and the maintenance of early pregnancy in humans[71]. Epithelial cells are the main source of endometrial CRH in the non-pregnant uterus[72]. The expression of the CRH gene in human endometrial cells can be induced by prostaglandin E2 (PGE_2)[73]. Intriguingly, human seminal plasma contains PGs, especially PGE_2, at levels up to 10,000 times higher than those observed in sites of chronic inflammation[74]. Thus, it is tempting to postulate that seminal plasma may also influence CRH expression in the female uterus via PGs.

Limitations of the study

In this study, we used *UGT305A1* knockdown males as venerose-depleted males. Although we confirmed that *UGT305A1* knockdown had no discernable effect on MAG morphology or SP content, which correlate with MAG maturation and function[42], it is still possible that *UGT305A1* knockdown affects other sexually transmitted molecules in addition to venerose. Nevertheless, the two main functions we ascribe to venerose, GSC proliferation and EHP expansion, are supported by highly compelling direct and indirect evidence. In the case of GSC proliferation, we directly validated the effect of venerose with in vivo rescue experiments achieved via synthetic venerose injection and ex vivo ovary culture experiments with synthetic venerose. For EHP expansion, which females exhibit roughly 90 min post-copulation, it was technically impossible to perform similar rescue experiments. This is because injecting venerose into flies requires anesthesia, which requires several hours to recover before any behavioral testing. Nevertheless, the indirect evidence supporting our conclusion that venerose regulates EHP expansion is compelling. In several in vitro and in vivo experiments, we established that synthetic venerose stimulates Dh44-PI neurons to secrete Dh44. There is also strong support in the literature[31] indicating that Dh44 secreted by Dh44-PI expands the EHP. Together, these points strongly suggest venerose regulates EHP expansion.

We found Dh44-PI neurons exhibited pronounced spontaneous activity with notable feeding state-dependent variation. Those of well-nourished females exhibited higher spontaneous activity than those of their starved counterparts. Hemolymph sugars like trehalose and glucose evoke robust calcium responses in Dh44-PI neurons[35], and well-nourished females exhibit higher blood sugar levels than starved females[75]. From this, we inferred that the increased spontaneous activity of well-nourished females must be at least partially influenced by the sugars of the internal milieu. It is important to note, however, that our data cannot prove a causal relationship between the spontaneous activity of Dh44-PI neurons and hemolymph sugar levels.

Our evidence that venerose-induced GSC proliferation requires Dh44 is very compelling. Dh44 can also stimulate GSC proliferation in the absence of venerose. For example, ovaries from virgin females showed GSC proliferation in response to Dh44 in vitro (Fig. 4e) and in vivo (Fig. 4i). However, female reproductive organs, such as the uterus, seminal vesicles, and spermathecae, are in contact with venerose in mated females. Thus, these tissues may be involved in signaling venerose reception and subsequent reproductive responses, including GSC proliferation. Future work will be required to address whether and how venerose interacts directly with female reproductive organs.

Methods

Flies

Flies were cultured on a standard diet (SD) containing dextrose, cornmeal, and yeast at room temperature in a 12 h:12 ho light:dark cycle. All behavioural assays were performed at 25 °C in Zeitgeber time (ZT) 5:00-11:00. Virgin males and females were collected at eclosion. Males were aged individually for 4–6 days; females were aged for 3–4 days in groups of 15–20. Starved flies were reared on 1% agar (Nacalai Tesque, 01056-15). All *Drosophila* stocks used in this study are shown in the key resources table. To create the *Dh44-R1* deficient allele (Dh44-R1^{-}), two guide RNAs (5′-gacagctcgcggtaccctggcgg, 5′-acatgggtctcctgcatccaggg) were inserted into pU6-BbsI-chiRNA plasmid (Addgene plasmid # 45946). This construct was then injected into M{vas-Cas9.S}ZH-2A (BDSC, 52669) to induce a defined microdeletion of 1261 bps spanning from TM1 to TM5 of Dh44-R1. The presence of microdeletion was vertified by genomic DNA PCR using primers: 5′-aagctggcttgtttgcctaa and 5′-catccgacatttttccgact; (PCR product size: control 2736 bps, mutant 1475 bps). UAS-Ugt305A1 was generated by amplifying a 1752 bps-long Ugt305A1 ORF with primers (5′-nnggtaccatgagggccttgtgtttact, 5′-nntctagattagtcttctttcttctcctcg) from the w^{1118} cDNA and cloning the KpnI-Ugt305A1-ORF-XbaI fragment into the SST13 vector. The resulting plasmid DNA was then injected into w^{1118} flies with a specific landing site on the second chromosome (VIE-72A) using the ΦC31 system.

Venerose extraction

To collect the male ejaculate for biochemical analysis, we used *Dh44-RNAi* females, which expel a white spermatophore-like sac made of semen and sperm shortly after mating[31]. The spermatophore-like sac or reproductive organs were homogenized in 10 μl of 0.1% formic acid. After spin-down (15,262 x g, 4 °C, 10 minutes), the supernatant was filtered by Zip-Tip C_{18} (Sigma, ZTC18S096) to remove protein and other hydrophobic substances. For the comparison of venerose contents in male reproductive tissues, dissected tissues of 10 males were collected and homogenized in 10 μl of 0.1% formic acid. After spin-down, 10 μl supernatant was mixed in 10 μl of 5.55 mM glucose as an internal standard. For the relative quantification of venerose in hemolymph, 1 μl hemolymph was mixed in 5 μl of 0.1% formic acid and 1 μl of 2.68 mM ^{13}C glucose as an internal standard. Hemolymph was collected, using a modified method described previously[76]. 30–40 female flies were punched on the thorax with a tungsten needle and were collected in a small 0.5 ml tube with a hole underneath. The small tube was then placed in 1.7 ml tubes and centrifuged (2649 x g, 4 °C, 5 min). To avoid contaminations from the male ejaculate that might remain in the females, we collected hemolymph from females 4 hours after mating when sperm ejection was completed.

Mass spectrometry and NMR spectroscopy

Mass spectrometric analyses were performed using a high mass accuracy, high resolution mass spectrometer (Q Exactive Plus mass spectrometer; Thermo Fisher Scientific, Bremen, Germany) and a linear trap mass spectrometer (LTQ; Thermo Fisher, Bremen, Germany) with a microspray ESI source operated in a full mass spectral acquisition mode for (+) and (−) MS scan in the mass range of m/z 100–500. The detailed MS parameter settings are shown in Supplementary Table 3. All mass spectrometry data is shown in Supplementary Data 3. NMR Spectroscopy– ^{1}H, ^{13}C, ^{31}P, and 2D-NMR experiments were performed using either a Varian Unity INOVA 500 or a Varian VNMRS 600 MHz NMR spectrometer. MAG extract collected from 200 males was analyzed with the NMR Spectroscopy. The ^{31}P-NMR signal intensities of MAG extract collected from 200 males were compared with those of 1 mM Na_3PO_4 standard to estimate the venerose content in MAG extract from a single male. The NMR analyses are shown in Supplementary Table 1 and Supplementary Fig. 2.

Carbohydrate-Active enZymes (CAZy) annotation

To annotate proteins with the CAZy domain, the peptide sequences of *Drosophila melanogaster* (BDGP6.32 assembly version, Ensembl database)[77] were mapped with profile hidden *Markov* models (HMM) of CAZy families, which were deposited at dbCAN, a CAZy domain HMM database[39], through HMMER v3.3, a homologs searching tool (hmmer.org) (e-values < 10-5) (See annotations in Supplementary Data 1).

QuantSeq 3′ mRNA-sequencing

Total RNA was extracted from 50–75 MAG for each sample using TRIZOL (Invitrogen, Korea) according to the manufacturer's instructions. The construction of library was performed using QuantSeq 3′ mRNA-Seq Library Prep Kit (Lexogen, Inc., Austria) according to the manufacturer's instructions. In brief, each 500 ng total RNA were prepared and an oligo-dT primer containing an Illumina-compatible sequence at its 5′ end was hybridized to the RNA and reverse transcription was performed. After degradation of the RNA template, second strand synthesis was initiated by a random primer containing an Illumina-compatible linker sequence at its 5′ end. The double-stranded library was purified by using magnetic beads to remove all reaction components. The library was amplified to add the complete adapter sequences required for cluster generation. The finished library is purified from PCR components. High-throughput sequencing was performed as single-end 75 sequencing using NextSeq 500 (Illumina, Inc., USA). QauntSeq 3′ mRNA-Seq Library generation and NGS run (>10 M read/sample) were performed by ebiogen Inc (Korea). Raw sequencing reads were mapped on the transcript sequence of *Drosophila melanogaster* (released version 6.42, FlyBase database)[78] using *kallisto* gene expression quantification program[79] to generate count value and transcript per million base pair (tpm) value for each transcript (see expression quantification table in Supplementary Data 2 and Table 2).

^{32}P-labeling and liquid scintillation spectrometry

For ^{32}P-labeling, flies were cultured with ^{32}P-labeling medium containing 5% sucrose, 5% yeast extract, 1% agar, and 10 μci/ml of Phosphorus-32 Raidonuclide, Monopotassium phosphate (NEX060001MC, perkinelmer)[80]. 10–15 males were collected immediately after eclosion and kept in a vial with ^{32}P-labeling medium. Five-day-old males were dissected in PBS, and male reproductive tissue including MAG and ejaculatory duct from three males were collected and homogenized in 20 μl of 0.1% formic acid. After spin-down (15,262 x g, 4 °C, 10 min), the supernatant was filtered by Zip-Tip C_{18} (Sigma, ZTC18S096) to remove protein and other hydrophobic substances in the same way as the venerose extraction protocol. The supernatant was mixed with 480 μl of PICO-FLUOR™ 40, a universal cocktail for solubilizing tissue samples. Heads of three males and ovaries of three mated females were collected in 20 μl of PBS, and mixed with 480 μl of PICO-FLUOR™ 40 without additional extraction steps. Disintegration per minute (DPM) values of solubilized samples or tissues were measured using a liquid scintillation counter, Hidex 300SI Super Low Level (HIDEX).

SP quantification

A chemiluminescent Western protein analyzer, Protein Simple Abby (Bio-techne), was used to measure SP levels. Each sample was prepared by homogenizing the reproductive tracts of 11 5-day-old males in 20 mL RIPA buffer (ThermoFisher, 89901) with protease inhibitors, adding 5X SDS loading buffer (Biosegment, SF2002), and heating at 98 °C for 5 minutes. Total protein levels were analyzed by the Bradford assay, and each sample was diluted to 0.2 mg/ml. For SP quantification, we used EZ Standard Pack 5 (Bio-Techne, PS-ST05EZ-8), rabbit anti-SP (1:400)[81] as the primary antibody, and an anti-rabbit secondary antibody (1X; Bio-Techne, 042–206). We then performed the analysis with 2–40 kDa separation capillary cartridges (Bio-Techne, SM-W012-01). For quantification of β-actin, lysates were analyzed with 12–230 kDa separating capillary cartridges (Bio-Techne, SM-W004-01) using EZ Standard Pack 1 (Bio-Techne, PS-ST01EZ-8), mouse anti-β-actin (1:50; Santa Cruz Biotechnology, sc-47778) as a primary antibody, and an anti-mouse secondary antibody (1X; Bio-Techne, 042-205). To confirm the specificity of the Western protein analysis for SP used in this study, we analyzed an SP-deficient mutant along with the appropriate controls (Supplementary Fig. 4d).

Egg-laying assay

We followed a previously described protocol[11]. Virgin w^{1118} females were aged in groups for 3 days after eclosion, and virgin males were aged individually for 5 days after eclosion. For mating, virgin females were paired individually with naïve males in 10-mm diameter chambers. Each female was allowed to lay eggs in SD vials for 7 days, and the number of eggs laid was counted every 24 h.

Sperm competition analysis

We modified a method described previously in ref. 82. Virgin *cn bw* females were aged in groups for 3 days after eclosion, and virgin males were aged individually for 5 days after eclosion. For defense assays, *cn bw* females were individually mated with test males in SD vials for 2 h. After 3 days, the females were individually re-mated with *cn bw* males for 12 hours in the same vial and transferred to a new SD vial. For the offense assays, *cn bw* females were mated with *cn bw* males and 3 days later with test males. Paternity was determined by allowing doubly mated females to lay eggs for 3 days and examining the eye color of the offspring.

Egg-to-pupa viability analysis

The mated females laid eggs in SD vials for 2 days, and the pupae that emerged were counted 5–6 days after egg laying.

Immunohistochemistry

To quantify the GSC number in germaria, ovaries were dissected in PBS (pH 7.4) and fixed for 20 min at room temperature with 4% paraformaldehyde in PBS. Fixed samples were washed three times in 0.1% PBST and blocked for 1 hour at room temperature with 5% normal goat serum in 0.1% PBST and then incubated with a primary antibody in blocking solution at 4 °C 24 to 48 h. Primary antibodies used in this study were mouse anti-Hts 1B1 [Developmental Studies Hybridoma Bank (DSHB); 1:50], rat anti–E-cadherin DCAD2 (DSHB; 1:50), chicken anti-GFP (Abcam; 1:8000), mouse anti-Lamin-C LC28.26 (DSHB; 1:50), guinea-pig anti-tj (1:5000)[83], and rabbit anti-pMad (Abcam; 1:1000). After washing, fluorophore (Alexa Fluor 488, 568, or 633)–conjugated secondary antibodies (Thermo Fisher Scientific) were used at a 1:200 dilution, and samples were incubated for 2 to 3 h at room temperature in 0.1% PBST. All samples were mounted with Vectashield. GSC numbers were determined on the basis of morphology and positioning of their anteriorly anchored spherical spectrosomes[84]. For GSC number

quantification, germaria for each experimental condition were derived from 15 to 20 females.

To examine GFP expression, ovaries, brains, and guts were dissected in PBS (pH 7.4) and fixed with 4% paraformaldehyde in PBS for 20 min at room temperature. After washing and blocking, the brains were incubated with rabbit anti-GFP antibody (1:1000; Invitrogen, A11122) for 24 h at 4 °C and with Alexa 488-conjugated goat anti-rabbit (1:1000; Invitrogen, A11008) and with Alexa 555 phalloidin (1:1000; Invitrogen, A34055) for 48 h at 4 °C.

To measure the intensity of Dh44, brains were dissected in PBS (pH 7.4) and fixed for 30 min at room temperature in 4% paraformaldehyde in PBS. After washing and blocking, the brains were incubated in primary antibody for 24 hours at 4 °C, and in secondary antibody for 24 h at 4 °C. The antibodies used were: rabbit anti-Dh44 (1:2000)[85] and Alexa 488-conjugated goat anti-rabbit (1:1000; Invitrogen, A11008). To quantify venerose-induced Dh44 secretion, the dissected brains were incubated with 100 μl of sugar-free adult hemolymph-like Ringer's saline (108 mM NaCl, 5 mM KCl, 2 mM $CaCl_2$, 8.2 mM $MgCl_2$, 4 mM $NaHCO_3$, 1 mM NaH_2PO_4, 5 mM HEPES)[86] with or without synthetic venerose for 30 minutes before fixation and anti-Dh44 staining. Tissues were mounted with Vectashield (Vector Laboratories, H-1000). Images were acquired with an LSM 700/Axiovert 200 M using a 40x lens (Zeiss) and processed in Image J[87]. For each sample, 15 confocal images of 5 μm thickness were captured to produce a Z-stacked image with averaged intensity.

Synthetic venerose

1-*O*-[4-*O*-(2-aminoethylphosphate)-β-$_D$-galactopyranosyl]-x-glycerol in a R and S isomer mix was custom synthesized by WuXi AppTec Co (China). Purity and yield of the synthetic scheme was shown in Supplementary Table 4.

Injection

Virgin females were aged in SD vials for 3 days. 0.1–0.8 nmol of venerose in 23 nl of sugar-free adult hemolymph-like Ringer's saline was injected into the abdomen of ice-anesthetized flies with a Nanoject II microinjector (Drummond). After injection, the flies were kept in SD vials until assay. For GSC number quantification, venerose was injected 24 hours before dissection.

Ex vivo organ culture

We modified a previously described protocol[14]. Virgin females were aged in groups for 3 days after eclosion. Organs were isolated in fly saline. Five pairs of ovaries were cultured in 1.5 ml tubes containing Schneider's *Drosophila* medium (SDM) supplemented with 15% fetal bovine serum and 1% penicillin-streptomycin with the addition of 1–10 mM venerose, 1 mM octopamine, or 1–10 nM Dh44. For co-culture experiments, five pairs of ovaries were co-cultured with five brains or five whole guts (including foregut, midgut, and hindgut but not the crop). Cultures were incubated at room temperature for 24 hours, and then samples were immunostained to quantify GSC numbers.

Calcium imaging

For ex vivo live calcium imaging, 4–5-day-old virgin females carrying P_{Dh44}-*Gal4* and *UAS-GCaMP6.0 m* were dissected under sugar-free adult hemolymph-like Ringer's saline. The brain was mounted on a cover slide with a 40 μl drop of saline bath containing 0.5 μM TTX and observed with a confocal microscope LSM 700/Axiovert 200 M with a 20x lens (Zeiss). The brain was recorded under GFP excitation light (470 nm) for a duration of 150 frames at 1 frame per 2 seconds. Subsequently, 10 μl of D-glucose or venerose in saline was added and the recording was resumed for an additional 750 frames. Image analyses and processing were performed using Image J and OriginPro9.1. F_O was calculated by averaging fluorescence values from 10 consecutive frames that showed baseline levels of GCaMP fluorescence. Ca^{2+} transients were defined as a peak reaching >50% of their maximum $\Delta F/F_O$ within a 10-frame-window. % Responders is the proportion of cells showing more than one Ca^{2+} transient. Max. peak amplitude was the defined as the maximum value of $\Delta F/F_O$. The oscillation number was the number of Ca^{2+} transients observed for each cell. The oscillation duration was calculated from the Ca^{2+} oscillation or peak with the maximum peak intensity in each cell and defined as the time interval between 50% of the rising phase and 50% of the decaying phase to the peak $\Delta F/F_O$. The area under the curve was calculated by integrating $\Delta F/F_O$ values over baseline after D-glucose or venerose application. Activity onset latency was defined as the time point when the first Ca^{2+} transient reached 50% of its peak $\Delta F/F_O$ in each cell. Cells that showed a strong baseline increase (> 50% ΔF) without a Ca^{2+} transient during the total recording period were excluded from the dataset (n = 226/514).

For in vivo live calcium imaging, a cold anesthetized virgin female carrying P_{Dh44}-*Gal4* and *UAS-GCaMP6.0 m* was fixed on a metal plate with light-curing instant adhesive (ThreeBond, TB1773E). A piece of fly head cuticle was cut and removed using the blade of a disposable needle (Kovax, 25 G 5/8") under sugar-free adult hemolymph-like Ringer's saline[86]. The brain was observed with an Axio Examiner A1 (Zeiss) equipped with a 40x water immersion lens (Zeiss, 421767-9970), a Luca^{EM} R 604 camera (ANDOR technology, DL-00419), and an LED light source (CoolLED, 244–1400). During recording, the brain was bathed in sugar-free adult hemolymph-like Ringer's saline. To normalize the fluorescent value for each fly, Dh44-PI neurons expressing both the Ca^{2+} indicator GCaMP6.0 m and the nucleus-targeted red fluorescent protein RedStinger were recorded under RFP excitation light (565 nm) for 60 frames (one frame per second) and then for an additional 100 frames under GFP excitation light (470 nm). The normalized relative fluorescence was calculated as $(F_{gi}- F_{bi})/F_r$, where F_{gi} represents GCaMP fluorescence of a cell body ROI (i.e., Region of interest) in the i^{th} frame, F_{bi} represents the GCaMP fluorescence value of a background ROI, and F_r represents the mean RFP fluorescence value of the first 60 frames. To calculate the area under the curve, the relative fluorescence values from all 5–6 visible cells in a brain preparation were averaged, integrated over 100 frames, and then normalized with the mean of the data from the fed group (n = 5). Image analyses and processing were done with Metamorph (Molecular Devices) and Exel (Microsoft).

Two-choice preference assay

We used a method described previously in ref. 88. Briefly, approximately 40 male flies 4–8 days old were starved for 18–22 h and then given a choice between 200 mM D-glucose (Sigma, 49139) and 200 mM L-glucose (Carbosynth, MG05247), each color-coded with tasteless food dyes (McCormick), for 2 hours. Food preference was scored as a percent preference index (% PI) as follows: %PI = ((# flies that ate food 1 + 0.5 * # flies ate both) − (# flies that ate food 2 + 0.5 * # flies that ate both)) / (total # flies that ate).

Ejaculate-holding period (EHP) analysis

For determining the EHP, which was defined as the period between the end of copulation and sperm ejection, virgin females were paired individually with naïve males in 10-mm diameter chambers. Immediately after copulation concluded (usually within 30 minutes), males were removed, and females were videotaped with a digital camcorder (SONY, DCR-SR47). EHP was normalized to yield ΔEHP by subtracting by the mean of the reference EHP. We assayed EHP in the absence of food because Dh44-PI neurons regulate feeding[35], and therefore mating-induced Dh44-PI activation (see main text) likely stimulates feeding activity. If females access food, it is possible for an interaction between Dh44-PI neurons and feeding activity to elongate the EHP.

Sperm storage analysis

Virgin females mated with naïve *protamine-GFP* males, the sperm heads of which express GFP, were frozen by transferring them to

−80 °C. Then, the seminal receptacles of females 6 hours post-mating were dissected in PBS and the number of sperm was manually counted using a fluorescence microscope (Olympus IX71).

Optogenetic silencing and activating experiments

For optogenetic silencing with GtACR1, freshly eclosed females were fed SD containing 1 mM all-*trans*-retinal (ATR) (Sigma, R2500) in constant darkness for 2–3 days. The flies then were exposed to light from a blue LED (460 nm, 24 μW/mm^2) for 18 hours prior to behavioral analysis. For optogenetic activation with CsCrimson, we used a custom-made light-activation chamber with a multi-channel WS2812 NeoPixel LED (Adafruit) light. The flies were exposed to light from a red LED (620–630 nm, 20 μW/mm^2) for 24 hours prior to the GSC counting assay.

Thermal activation experiments

For thermal activation with dTrpA1, freshly eclosed females were stored in SD vials for 1 day at 20 °C and then transferred to 20 °C or 30 °C for 2 days prior to behavioral analysis.

Single-nucleus RNA transcriptome analysis

The snRNA-seq datasets and cell type metadata for testis and male reproductive glands were obtained from the Fly Cell Atlas (flycellatlas.org). The loom files (s_fca_biohub_testis_10x_ss2.loom, s_fca_biohub_male_reproductive_glands_10x_ss2.loom) were downloaded and converted into Seurat objects. These Seurat objects were then normalized and scaled according to the Seurat pipeline[89].

Statistics and Reproducibility

Experimental flies and genetic controls were tested under the same conditions, and data were collected from at least two independent experiments. For behavioral assays, sample size was determined by previous studies[11,14,31,35,82,88]. All flies were collected randomly from the same population. Age-matched flies were used for all experiments. To reduce bias, the data were measured by multiple investigators without any information about experimental conditions. Statistical analyses were performed using GraphPad Prism Software version 8.00 (GraphPad Software) or Stata 17 (StataCorp. 2021). For one-way ANOVA, the Bonferroni post-hoc analysis was used if at least 50% of the comparison groups passed the Shapiro-Wilk normality test. Kruskal-Wallis tests with Dunn post-hoc analyses were used otherwise. Two-way ANOVA was used if at least 50% of the comparison groups passed the Shapiro-Wilk normality test. Robust ANOVA was used otherwise. For comparisons between two groups, unpaired *t*-tests were used if at least 50% of the comparison groups passed the Shapiro-Wilk normality test. Mann-Whitney tests were used otherwise. The exact *p*-values and statistical methods used are shown in the figure legends and in Supplementary Data 4.

Reporting summary

Further information on research design is available in the Nature Portfolio Reporting Summary linked to this article.

Data availability

The RNA-seq data from male reproductive glands have been deposited in the NCBI Sequence Read Archive under accession code PRJNA1140569. All data presented in figures and mass spectrometry data generated in this study are provided in Source Data files and Supplementary Data 4, respectively. Source data are provided with this paper.

Code availability

The codes used for the data analysis for QuantSeq 3′ mRNA-seq and snRNA-seq have been deposited in Zenodo (https://doi.org/10.5281/zenodo.13643789).

References

1. Robertson, S. A. & Sharkey, D. J. Seminal fluid and fertility in women. *Fertil. Steril.* **106**, 511–519 (2016).
2. Samanta, L., Parida, R., Dias, T. R. & Agarwal, A. The enigmatic seminal plasma: a proteomics insight from ejaculation to fertilization. *Reprod. Biol. Endocrinol.* **16**, 41 (2018).
3. Poiani, A. Complexity of seminal fluid: a review. *Behav. Ecol. Sociobiol.* **60**, 289–310 (2006).
4. Gonzales, G. F. & Villena, A. True corrected seminal fructose level: a better marker of the function of seminal vesicles in infertile men. *Int J. Androl.* **24**, 255–260 (2001).
5. Avila, F. W., Sirot, L. K., LaFlamme, B. A., Rubinstein, C. D. & Wolfner, M. F. Insect Seminal Fluid Proteins: Identification and Function. *Annu. Rev. Entomol.* **56**, 21–40 (2011).
6. Wigby, S. et al. The *Drosophila* seminal proteome and its role in postcopulatory sexual selection. *Philos. Trans. R. Soc. B* **375**, 20200072 (2020).
7. Chen, P. S. et al. A male accessory gland peptide that regulates reproductive behavior of female D. melanogaster. *Cell* **54**, 291–298 (1988).
8. Kubli, E. Sex-peptides: seminal peptides of the Drosophila male. *Cell. Mol. Life Sci. (CMLS)* **60**, 1689–1704 (2003).
9. Delbare, S. Y. N. et al. Time series transcriptome analysis implicates the circadian clock in the *Drosophila melanogaster* female's response to sex peptide. *Proc. Natl Acad. Sci. USA.* **120**, e2214883120 (2023).
10. Ameku, T. & Niwa, R. Mating-Induced Increase in Germline Stem Cells via the Neuroendocrine System in Female Drosophila. *PLoS Genet.* **12**, e1006123 (2016).
11. Zhang, C., Kim, A. J., Rivera-Perez, C., Noriega, F. G. & Kim, Y.-J. The insect somatostatin pathway gates vitellogenesis progression during reproductive maturation and the post-mating response. *Nat. Commun.* **13**, 969 (2022).
12. Kim, Y.-J. & Zhang, C. Neuronal Mechanisms that Regulate Vitellogenesis in the Fruit Fly. *Korean J. Appl. Entomol.* **61**, 109–115 (2022).
13. Xie, T. & Spradling, A. C. A Niche Maintaining Germ Line Stem Cells in the *Drosophila* Ovary. *Science* **290**, 328–330 (2000).
14. Yoshinari, Y. et al. Neuronal octopamine signaling regulates mating-induced germline stem cell increase in female Drosophila melanogaster. *eLife* **9**, e57101 (2020).
15. Ameku, T. et al. Midgut-derived neuropeptide F controls germline stem cell proliferation in a mating-dependent manner. *PLoS Biol.* **16**, e2005004 (2018).
16. Steele, R. H. Courtship feeding in Drosophila subobscura. I. The nutritional significance of courtship feeding. *Anim. Behav.* **34**, 1087–1098 (1986).
17. Lack, D. Courtship Feeding in Birds. *Auk* **57**, 169–178 (1940).
18. Alley, T. R., Brubaker, L. W. & Fox, O. M. Courtship Feeding in Humans?: The Effects of Feeding versus Providing Food on Perceived Attraction and Intimacy. *Hum. Nat.* **24**, 430–443 (2013).
19. Brown, W. D. & Barry, K. L. Sexual cannibalism increases male material investment in offspring: quantifying terminal reproductive effort in a praying mantis. *Proc. R. Soc. B.* **283**, 20160656 (2016).
20. Neumann, R. & Schneider, J. M. Males sacrifice their legs to pacify aggressive females in a sexually cannibalistic spider. *Anim. Behav.* **159**, 59–67 (2020).
21. Chapman, T. Seminal fluid-mediated fitness traits in Drosophila. *Heredity* **87**, 511–521 (2001).
22. Markow, T. A., Coppola, A. & Watts, T. D. How *Drosophila* males make eggs: it is elemental. *Proc. R. Soc. Lond. B* **268**, 1527–1532 (2001).
23. Kamimura, Y., Yoshizawa, K., Lienhard, C., Ferreira, R. L. & Abe, J. Evolution of nuptial gifts and its coevolutionary dynamics with male-like persistence traits of females for multiple mating. *BMC Ecol. Evol.* **21**, 164 (2021).

24. Steele, R. H. Courtship feeding in Drosophila subobscura. II. Courtship feeding by males influences female mate choice. *Anim. Behav.* **34**, 1099–1108 (1986).
25. Sakaluk, S. K. Male Crickets Feed Females to Ensure Complete Sperm Transfer. *Science* **223**, 609–610 (1984).
26. Albo, M. J., Bilde, T. & Uhl, G. Sperm storage mediated by cryptic female choice for nuptial gifts. *Proc. R. Soc. B.* **280**, 20131735 (2013).
27. Fedina, T. Y. Cryptic female choice during spermatophore transfer in Tribolium castaneum (Coleoptera: Tenebrionidae). *J. Insect Physiol.* **53**, 93–98 (2007).
28. Toft, S. & Albo, M. J. Optimal numbers of matings: the conditional balance between benefits and costs of mating for females of a nuptial gift-giving spider. *J. Evol. Biol.* **28**, 457–467 (2015).
29. Eberhard, W. G. Evidence for Widespread Courtship During Copulation in 131 Species of Insects and Spiders, and Implications for Cryptic Female Choice. *Evolution* **48**, 711 (1994).
30. Lüpold, S. et al. Female mediation of competitive fertilization success in *Drosophila melanogaster*. *Proc. Natl Acad. Sci. USA.* **110**, 10693–10698 (2013).
31. Lee, K.-M. et al. A Neuronal Pathway that Controls Sperm Ejection and Storage in Female Drosophila. *Curr. Biol.* **25**, 790–797 (2015).
32. Davies, N. B. Polyandry, cloaca-pecking and sperm competition in dunnocks. *Nature* **302**, 334–336 (1983).
33. Pizzari, T. & Birkhead, T. R. Female feral fowl eject sperm of subdominant males. *Nature* **405**, 787–789 (2000).
34. Snook, R. R. & Hosken, D. J. Sperm death and dumping in Drosophila. *Nature* **428**, 939–941 (2004).
35. Dus, M. et al. Nutrient Sensor in the Brain Directs the Action of the Brain-Gut Axis in Drosophila. *Neuron* **87**, 139–151 (2015).
36. Oh, Y. et al. Periphery signals generated by Piezo-mediated stomach stretch and Neuromedin-mediated glucose load regulate the Drosophila brain nutrient sensor. *Neuron* **109**, 1979–1995.e6 (2021).
37. Chen, P. S., Fales, H. M., Levenbook, L., Sokoloski, E. A. & Yeh, H. J. C. Isolation and characterization of a unique galactoside from male Drosophila melanogaster. *Biochemistry* **16**, 4080–4085 (1977).
38. Wainwright, S. M. et al. *Drosophila* Sex Peptide controls the assembly of lipid microcarriers in seminal fluid. *Proc. Natl Acad. Sci. Usa.* **118**, e2019622118 (2021).
39. Yin, Y. et al. dbCAN: a web resource for automated carbohydrate-active enzyme annotation. *Nucleic Acids Res.* **40**, W445–W451 (2012).
40. Drula, E. et al. The carbohydrate-active enzyme database: functions and literature. *Nucleic Acids Res.* **50**, D571–D577 (2022).
41. Coutinho, P. M., Deleury, E., Davies, G. J. & Henrissat, B. An Evolving Hierarchical Family Classification for Glycosyltransferases. *J. Mol. Biol.* **328**, 307–317 (2003).
42. Ruhmann, H., Wensing, K. U., Neuhalfen, N., Specker, J.-H. & Fricke, C. Early reproductive success in *Drosophila* males is dependent on maturity of the accessory gland. *Behav. Ecol.* **27**, 1859–1868 (2016).
43. Li, H. et al. Fly Cell Atlas: A single-nucleus transcriptomic atlas of the adult fruit fly. *Science* **375**, eabk2432 (2022).
44. Mattei, A. L., Riccio, M. L., Avila, F. W. & Wolfner, M. F. Integrated 3D view of postmating responses by the *Drosophila melanogaster* female reproductive tract, obtained by micro-computed tomography scanning. *Proc. Natl Acad. Sci. Usa.* **112**, 8475–8480 (2015).
45. Spradling, A., Fuller, M. T., Braun, R. E. & Yoshida, S. Germline Stem Cells. *Cold Spring Harb. Perspect. Biol.* **3**, a002642–a002642 (2011).
46. Miscopein Saler, L. et al. The Bric-à-Brac BTB/POZ transcription factors are necessary in niche cells for germline stem cells establishment and homeostasis through control of BMP/DPP signaling in the Drosophila melanogaster ovary. *PLoS Genet.* **16**, e1009128 (2020).
47. LaFever, L. & Drummond-Barbosa, D. Direct Control of Germline Stem Cell Division and Cyst Growth by Neural Insulin in *Drosophila*. *Science* **309**, 1071–1073 (2005).
48. Slaidina, M., Banisch, T. U., Gupta, S. & Lehmann, R. A single-cell atlas of the developing *Drosophila* ovary identifies follicle stem cell progenitors. *Genes Dev.* **34**, 239–249 (2020).
49. Drummond-Barbosa, D. Local and Physiological Control of Germline Stem Cell Lineages in *Drosophila melanogaster*. *Genetics* **213**, 9–26 (2019).
50. Luo, L., Siah, C. K. & Cai, Y. Engrailed acts with Nejire to control *decapentaplegic* expression in the *Drosophila* ovarian stem cell niche. *Development* **144**, 3224–3231 (2017).
51. Weaver, L. N., Ma, T. & Drummond-Barbosa, D. Analysis of Gal4 Expression Patterns in Adult *Drosophila* Females. *G3 Genes|Genomes|Genet.* **10**, 4147–4158 (2020).
52. Tayler, T. D., Pacheco, D. A., Hergarden, A. C., Murthy, M. & Anderson, D. J. A neuropeptide circuit that coordinates sperm transfer and copulation duration in *Drosophila*. *Proc. Natl Acad. Sci. Usa.* **109**, 20697–20702 (2012).
53. Macartney, E. L., Crean, A. J., Nakagawa, S. & Bonduriansky, R. Effects of nutrient limitation on sperm and seminal fluid: a systematic review and meta-analysis. *Biol. Rev.* **94**, 1722–1739 (2019).
54. Folk, D. G., Han, C. & Bradley, T. J. Water acquisition and partitioning in *Drosophila melanogaster*: effects of selection for desiccation-resistance. *J. Exp. Biol.* **204**, 3323–3331 (2001).
55. Serguera, C., Triaca, V., Kelly-Barrett, J., Banchaabouchi, M. A. & Minichiello, L. Increased dopamine after mating impairs olfaction and prevents odor interference with pregnancy. *Nat. Neurosci.* **11**, 949–956 (2008).
56. Kocher, S. D., Tarpy, D. R. & Grozinger, C. M. The effects of mating and instrumental insemination on queen honey bee flight behaviour and gene expression. *Insect Mol. Biol.* **19**, 153–162 (2010).
57. Liu, P.-C. & Hao, D.-J. Behavioural and transcriptional changes in post-mating females of an egg parasitoid wasp species. *R. Soc. open sci.* **6**, 181453 (2019).
58. Piper, M. D. W. et al. A holidic medium for Drosophila melanogaster. *Nat. Methods* **11**, 100–105 (2014).
59. Tryjanowski, P. & Hromada, M. Do males of the great grey shrike, Lanius excubitor, trade food for extrapair copulations? *Anim. Behav.* **69**, 529–533 (2005).
60. Salzer, D. W. & Larkin, G. J. Impact of courtship feeding on clutch and third-egg size in glaucous-winged gulls. *Anim. Behav.* **39**, 1149–1162 (1990).
61. Reaume, C. J. & Sokolowski, M. B. The nature of Drosophila melanogaster. *Curr. Biol.* **16**, R623–R628 (2006).
62. Wedell, N. Spermatophore Size in Bushcrickets: Comparative Evidence for Nuptial Gifts as a Sperm Protection Device. *Evolution* **47**, 1203 (1993).
63. Voight, J. R. Differences in Spermatophore Availability Among Octopodid Species (Cephalopoda: Octopoda). *Malacologia* **51**, 143–153 (2009).
64. Scolari, F. et al. The Spermatophore in Glossina morsitans morsitans: Insights into Male Contributions to Reproduction. *Sci. Rep.* **6**, 20334 (2016).
65. Swanson, W. J., Clark, A. G., Waldrip-Dail, H. M., Wolfner, M. F. & Aquadro, C. F. Evolutionary EST analysis identifies rapidly evolving male reproductive proteins in *Drosophila*. *Proc. Natl Acad. Sci. USA.* **98**, 7375–7379 (2001).
66. Haerty, W. et al. Evolution in the Fast Lane: Rapidly Evolving Sex-Related Genes in Drosophila. *Genetics* **177**, 1321–1335 (2007).
67. Findlay, G. D., Yi, X., MacCoss, M. J. & Swanson, W. J. Proteomics Reveals Novel Drosophila Seminal Fluid Proteins Transferred at Mating. *PLoS Biol.* **6**, e178 (2008).
68. Okamoto, S. et al. Activation of AMPK-Regulated CRH Neurons in the PVH is Sufficient and Necessary to Induce Dietary Preference for Carbohydrate over Fat. *Cell Rep.* **22**, 706–721 (2018).

69. Breen, K. & Karsch, F. New insights regarding glucocorticoids, stress and gonadotropin suppression. *Front. Neuroendocrinol.* **27**, 233–245 (2006).
70. Fourman, L. T. & Fazeli, P. K. Neuroendocrine Causes of Amenorrhea—An Update. *J. Clin. Endocrinol. Metab.* **100**, 812–824 (2015).
71. Kalantaridou, S. N. et al. Corticotropin-releasing hormone, stress and human reproduction: an update. *J. Reprod. Immunol.* **85**, 33–39 (2010).
72. Makrigiannakis, A. et al. The corticotropin-releasing hormone (CRH) in normal and tumoral epithelial cells of human endometrium. *M.* (1995).
73. Dibbs, K. I., Anteby, E., Mallon, M. A., Sadovsky, Y. & Adler, S. Transcriptional Regulation of Human Placental Corticotropin-Releasing Factor by Prostaglandins and Estradiol1. *Biol. Reprod.* **57**, 1285–1292 (1997).
74. Sales, K. J., Adefuye, A., Nicholson, L. & Katz, A. A. CCR5 expression is elevated in cervical cancer cells and is up-regulated by seminal plasma. *MHR: Basic Sci. Reprod. Med.* **20**, 1144–1157 (2014).
75. Cao, H., Wiemerslage, L., Marttila, P. S. K., Williams, M. J. & Schiöth, H. B. Bis-(2-ethylhexyl) Phthalate Increases Insulin Expression and Lipid Levels in *Drosophila melanogaster*. *Basic Clin. Pharma Tox* **119**, 309–316 (2016).
76. Haselton, A. T. & Fridell, Y.-W. C. Insulin Injection and Hemolymph Extraction to Measure Insulin Sensitivity in Adult Drosophila melanogaster. *J. Vis. Exp.* **52**, e2772 (2011).
77. Yates, A. D. et al. Ensembl 2020. *Nucleic Acids Res.* **48**, D682–D688 (2019).
78. Gramates, L. S. et al. FlyBase: a guided tour of highlighted features. *Genetics* **220**, iyac035 (2022).
79. Bray, N. L., Pimentel, H., Melsted, P. & Pachter, L. Near-optimal probabilistic RNA-seq quantification. *Nat. Biotechnol.* **34**, 525–527 (2016).
80. Lee, W. R., Sega, G. A. & Alford, C. F. Mutations produced by transmutation of phosphorus-32 to sulfur-32 within Drosophila DNA. *Proc. Natl Acad. Sci. USA.* **58**, 1472–1479 (1967).
81. Misra, S. & Wolfner, M. F. Drosophila seminal sex peptide associates with rival as well as own sperm, providing SP function in polyandrous females. *eLife* **9**, e58322 (2020).
82. Immarigeon, C. et al. Identification of a micropeptide and multiple secondary cell genes that modulate *Drosophila* male reproductive success. *Proc. Natl Acad. Sci. USA.* **118**, e2001897118 (2021).
83. Hoshino, R., Sano, H., Yoshinari, Y., Nishimura, T. & Niwa, R. Circulating fructose regulates a germline stem cell increase via gustatory receptor–mediated gut hormone secretion in mated *Drosophila*. *Sci. Adv.* **9**, eadd5551 (2023).
84. Ables, E. T. & Drummond-Barbosa, D. The Steroid Hormone Ecdysone Functions with Intrinsic Chromatin Remodeling Factors to Control Female Germline Stem Cells in Drosophila. *Cell Stem Cell* **7**, 581–592 (2010).
85. Cabrero, P. et al. The *Dh* gene of *Drosophila melanogaster* encodes a diuretic peptide that acts through cyclic AMP. *J. Exp. Biol.* **205**, 3799–3807 (2002).
86. Croset, V., Schleyer, M., Arguello, J. R., Gerber, B. & Benton, R. A molecular and neuronal basis for amino acid sensing in the Drosophila larva. *Sci. Rep.* **6**, 34871 (2016).
87. Schneider, C. A., Rasband, W. S. & Eliceiri, K. W. NIH Image to ImageJ: 25 years of image analysis. *Nat. Methods* **9**, 671–675 (2012).
88. Dus, M., Min, S., Keene, A. C., Lee, G. Y. & Suh, G. S. B. Taste-independent detection of the caloric content of sugar in *Drosophila*. *Proc. Natl Acad. Sci. USA.* **108**, 11644–11649 (2011).
89. Hao, Y. et al. Dictionary learning for integrative, multimodal and scalable single-cell analysis. *Nat. Biotechnol.* **42**, 293–304 (2024).

Acknowledgements

We thank Drs. H. I. Jung (Yonsei University) and S. J. Moon (Yonsei University) for advice on statistical analysis, Drs. M-R. Song (GIST) and Y. Jun (GIST) for insightful discussions, and K. Kim (GIST) for the graphical illustrations. We also thank Dr. M. Dus (New York University), B. Park (GIST) and S-H. Kim (GIST) for excellent technical assistance. The term venerose was suggested by Dr. Jennifer M. Widmer and Dr. Alexandre Widmer of Giez, Switzerland. This work was supported by the Japan Society for the Promotion of Science (JSPS) KAKEN grant (# 22H00414) to R.N., the GIST Research Institute (GRI) 2023 to Y-J.K., and the National Research Foundation of Korea (NRF) Basic Science Research Program grants (NRF-2018R1A2A1A05079359, NRF-2019R1A4A1029724, NRF-2022M3E5E8081194, NRF-2022R1A2C3008091) supported by the Ministry of Science, ICT and Future Planning to Y-J.K. Stocks were obtained from the Korea *Drosophila* Resource Center (NRF-2022M3H9A1085169), the Bloomington *Drosophila* Stock Center, and the Vienna *Drosophila* Resource Center.

Author contributions

Conceptualization: S-J.K., K-M.L., and Y-J.K.; Methodology: S-J.K, K-M.L., S.H.P., J-I.K., S.L., and Z-Y.P.; Investigation: S-J.K., K-M.L., S.H.P., T.Y., I.S., F.R., R.H., M.Y., C.Z., and S.L.; Visualization: S-J.K.; Writing—original draft: S-J.K., K-M.L., Y-J.K.; Writing—review & editing: S-J.K., G.S.B.S., R.N., Y-J.K.; Funding Acquisition: R.N., Y-J.K.; Supervision: Y-J.K.

Competing interests

The authors declare no competing interests.

Additional information

Supplementary information The online version contains supplementary material available at https://doi.org/10.1038/s41467-024-52807-3.

Correspondence and requests for materials should be addressed to Young-Joon Kim.

Peer review information *Nature Communications* thanks Daisuke Yamamoto and the other, anonymous, reviewer(s) for their contribution to the peer review of this work. A peer review file is available.